จุฬาลงกรณ์มหาวิทยาลัย
ทุนวิจัย
กองทุนรัชดาภิเษกสมโภช

รายงานวิจัย

การกลายพันธุ์ยีนไซโคลเดกซ์ทรินกลูคาโนแทรนส์เฟอเรส ที่มีผลต่อความทนร้อนของเอนไซม์

โดย
วิเชียร ริมพณิชยกิจ
เรวดี สิริธัญญานนท์

พฤษภาคม 2549

จุฬาลงกรณ์มหาวิทยาลัย
ทุนวิจัย
กองทุนรัชดาภิเษกสมโภช

รายงานวิจัย

การกลายพันธุ์ยีนไซโคลเดกซ์ทรินกลูคาโนแทรนส์เฟอเรส ที่มีผลต่อความทนร้อนของเอนไซม์

โดย

วิเชียร ริมพณิชยกิจ
เรวดี สิริธัญญานนท์

พฤษภาคม 2549

ACKNOWLEDGEMENTS

My appreciation is expressed to Rajadapiseksompote Research Fund from Chulalongkorn University for supporting this research.

Special thanks are expressed to Hematology Section, National Institute of Health, Department of Medical Sciences, for assistance in DNA sequencing.

Sincere thanks are extended to all the reviewers for their comments and suggestion. The helps of the staff members at the Office of Academic Affairs are greatly appreciated.

ชื่อโครงการวิจัย การกลายพันธุ์ยีนไซโคลเดกซ์ทรินกลูคาโนแทรนส์เฟอเรสที่มีผลต่อความทนร้อนของเอนไซม์

ชื่อผู้วิจัย วิเชียร ริมพณิชยกิจ และเรวดี สิริธัญญานนท์

เดือนและปีที่ทำวิจัยเสร็จ พฤษภาคม 2549

บทคัดย่อ

ไซโคลเดกซ์ทริน (CD) เป็นออลิโกแซ็กคาไรด์ที่ประกอบด้วยกลูโคส 6, 7 และ 8 หน่วย เรียกว่า α-, β- และ γ-ไซโคลเดกซ์ทริน ตามลำดับ CD เป็นผลิตภัณฑ์ที่เกิดจากการย่อยแป้งของไซโคลเดกซ์ทรินกลูคาโนแทรนส์เฟอเรส (CGTase) และใช้เป็นโมเลกุลพาหะ สำหรับประยุกต์ใช้ต่าง ๆ ในอุตสาหกรรม CGTase ประกอบด้วยโครงสร้าง 5 โดเมน คือ A, B, C, D และ E โดเมน A/B เป็นโดเมนเร่งปฏิกิริยา ขณะที่โดเมนอื่นทำหน้าที่ประกอบอื่น ๆ การผลิต CD ทางการค้าต้องนำแป้งมาย่อยด้วยเอนไซม์แอมิเลสที่อุณหภูมิสูง ก่อนที่จะนำมาบ่มกับ CGTase ที่อุณหภูมิต่ำกว่ามาก CGTase ทนร้อนจึงเป็นประโยชน์ต่อการผลิต CD อย่างมีประสิทธิภาพ จากการเปรียบเทียบลำดับกรดอะมิโน ระหว่าง *Bacillus circulans* A11 กับแบคทีเรียทนร้อน พบว่า มีบริเวณที่แตกต่างอย่างชัดเจน 4 บริเวณ คือ บริเวณที่ I, II, III และ IV ที่ตำแหน่ง 89-94, 265-271, 333-339 และ 538-540 (ตำแหน่งกรดอะมิโนของ CGTase จาก *Bacillus circulans* A11) โดยบริเวณที่เกี่ยวข้อง I-III อยู่บนโดเมน A/B การศึกษาครั้งนี้ได้กลายพันธุ์บริเวณทั้งสามบน β-CGTase จาก *B. circulans* A11 ให้คล้ายกับลำดับกรดอะมิโนของ CGTase ทนร้อน โดยวิธี unique site elimination (USE) mutagenesis ได้พลาสมิดมิวแทนต์ pRS1, 2 และ 3 ที่มีบริเวณกลายพันธุ์ I, II และ III ตามลำดับ แล้วทำการสร้างรีคอมบิแนนท์พลาสมิดที่มีตำแหน่งกลายพันธุ์ผสมต่าง ๆ ของทั้งสามตำแหน่ง จากนั้นทำการศึกษา dextrinizing activity, thermostabilty และ CD forming activity ของเอนไซม์มิวแทนต์ เพื่อตรวจสอบว่าบริเวณเหล่านี้มีผลต่อเสถียรภาพการทนร้อนของ CGTase อย่างไร พบว่า บริเวณกลายพันธุ์ทั้งสามทำให้มี dextrinizing activity สูงขึ้น มีอุณหภูมิเหมาะสมลดลง และไม่ได้ทำให้เสถียรภาพทนร้อนเพิ่มขึ้น มิวแทนต์ CGTase ทุกตัวสามารถสร้าง CD ได้ ทุกตัว ยกเว้นตัวเดียว มีความจำเพาะต่อการสร้างผลิตภัณฑ์เปลี่ยนแปลงไป

Project Title Mutagenesis of cyclodextrin glucanotransferase gene that affects themostability of the enzyme

Names of the Investigators Vichien Rimphanitchayakit and Raevadee Siritunyanont

Year May, 2004

ABSTRACT

Cyclodextrins are cyclic oligosaccharides of 6, 7 and 8 glucose units, called α-, β- and γ-cyclodextrins (CDs), respectively. CDs are the products of enzymatic conversion of starch and related substrates by cyclodextrin glucanotransferases (CGTases), and are useful carrier molecules for several applications in industries. The CGTase consists of 5 domains, A, B, C, D and E. Domains A/B are the central catalytic domains while others perform accessory functions. The commercial production of CDs required that the starch be liquefied at high temperature before the CGTase reaction at much lower temperature. Thermostable CGTase would, therefore, be useful for efficient production of CDs. By using amino acid sequence comparison between the *Bacillus circulans* A11 CGTase and the thermostable CGTases, four major different regions I, II, III and IV were found at position 89-94, 265-271, 333-339, and 538-540 (*B. circulans* A11 CGTase numbering), respectively. The relevant regions I-III were located in domains A/B. In this study, these three regions in β-CGTase from *Bacillus circulans* A11 were mutated in favor of the thermostable CGTase sequences using the unique site elimination (USE) mutagenesis method. The mutant plasmids, pRS1, 2 and 3 that have the mutation region I, II, and III, respectively, were obtained. Then, the mutant plasmids containing the various combinations of the 3 mutation regions were constructed. The dextrinizing activity, thermostability and CD-forming activity of the mutant enzymes from these clones were studied in order to determine whether how these different regions affect the thermostability of CGTase. We found that all the three mutation regions gave rise to an increase in dextrinizing activity, a decrease in optimum temperature and no increase in thermostability. All CGTase mutants were active in CD-forming activity; all but one with altered product specificity.

CONTENTS

Page

ACKNOWLEDGEMENTS ii
THAI ABSTRACT iii
ENGLISH ABSTRACT iv
CONTENTS v
LIST OF TABLES vii
LIST OF FIGURES viii
ABBREVIATION x
CHAPTER I INTRODUCTION 1
1.1 Application of cyclodextrins 3
1.2 Commercial production of cyclodextrins using CGTases 5
1.3 Three-dimensional structure of CGTase 6
1.4 CGTase reaction and its catalytic mechanism 9
1.5 Thermostability of CGTases 11
1.6 Protein engineering for CGTase thermostability 14
1.7 Scope of this study 15
CHAPTER II MATERIALS AND METHODS 16
2.1 Equipments 16
2.2 Chemicals 16
2.3 Bacterial strains 18
2.4 Plasmid vector 18
2.5 Enzymes 18
2.6 Media preparation 19
2.7 General techniques in genetic engineering 19
2.7.1 Preparation of competent cells 19
2.7.2 Electroporation 20
2.7.3 Plasmid preparation (alkaline lysis method) 20
2.7.4 Agarose gel electrophoresis 20
2.7.5 Extraction of the DNA fragment from the agarose gel 21

2.7.6 Preparation of single-stranded plasmid....21
2.7.7 Phosphorylation of oligonucleotide primers....22
2.8 Mutagenesis of β-CGTase gene using the USE (Unique Site Elimination) procedure....22
2.9 Construction of the recombinant plasmids containing various combination of the mutant regions....24
2.10 Detection of the mutant CGTase activity....25
2.10.1 Dextrinizing activity....25
2.10.2 CGTase thermostability testing....26
2.10.3 Cyclodextrin-forming activity....26
2.11 Protein determination....27
CHAPTER III RESULTS....28
3.1 Amino acid sequence comparison and the design of mutagenic primers....28
3.2 Mutagenesis of CGTase gene from *Bacillus circulans* A11....31
3.3 DNA sequencing determination of the mutation regions....33
3.4 Construction of the mutant CGTases....34
3.5 The activities of the mutant CGTases....37
3.5.1 Halo zone on LB-starch agar....37
3.5.2 Dextrinizing activity assay at various temperatures....39
3.5.3 Thermostability of the CGTases....41
3.5.4 Cyclodextrin forming activity....42
CHAPTER IV DISCUSSION....46
CHAPTER V CONCLUSION....55
REFERENCES....56
APPENDICES....62

LIST OF TABLES

Table **Page**

1.1. Characteristics of α-, β-, and γ-CDs.....5

1.2. Some characteristics of the mesophilic and thermophilic CGTases.....11

3.1. Dextrinizing activity assay of wild-type and mutant CGTases 40

3.2. Specific activities of wild-type and mutant CGTases in the thermostability assay.....41

3.3. Cyclodextrin-forming activity of the CGTases.....45

LIST OF FIGURES

Figure **Page**

1.1. Schematic representation of the action of starch-processing enzymes 2
1.2. Structures and properties of cyclodextrins 5
1.3. Comparison of the three dimensional structures of α-amylase and CGTase 7
1.4. Domain level organization of starch-degradating enzymes 7
1.5. Schematic representation of the hydrogen bonds between the *B. circulans* strain 251 CGTase and a maltononaose inhibitor bound at each subsite of the active site 8
1.6. Schematic representation of the CGTase-catalysed reactions 10
1.7. The CGTase reaction mechanism 10
1.8. The three dimensional structures of two mesophilic CGTases 12
1.9. The three dimensional structures of two thermostable CGTases 12
1.10. Alignment of amino acid sequences of mesophilic and thermophilic CGTases 13
2.1. The mutageneic oligonucleotides used to produce the mutations in the USE mutagenesis procedure 23
2.2. Schematic diagram of USE mutagenesis protocol 24
3.1. Amino acid sequence comparison of the various CGTases 29
3.2. The design of oligonucleotides used in the USE mutagenesis procedure 31
3.3. Restriction digestion of pRS1A, 1B, 2, and 3 32
3.4. The mutated plasmids, pRS1A, 1B, 2 and 3 32
3.5. Nucleotide sequencing of mutant regions I_A (A), I_B (B), II (C), and III (D) in pRS1A, 1B, 2 and 3, respectively 33
3.6. Summary of the mutant CGTase conctructs 35
3.7. Restriction digestion of pRS4A, 4B, 5, 6, 7A and 7B 36
3.8. Restriction digestion of pRS8A, 8B, 9, 10A and 10B 37
3.9. Iodine test for dextrinizing activity of wild type and mutant CGTases 38
3.10. Summary of the iodine test for dextrinizing activity of the wild type and the mutant CGTases 39

3.11. Dextrinizing activity assay of the wild-type and mutant CGTases.....40
3.12. Thermostability of the wild-type and mutant CGTases.....41
3.13. HPLC profiles of cyclodextrins formed by the wild type and mutant CGTases.....43
4.1. Location of the three mutations regions relative to the binding subsites, presented by the maltononaose.....49

ABBREVIATION

BSA	Bovine serum albumin
CD	Cyclodextrin
CGTase	Cyclodextrin glucanotransferase
ºC	Degree Celsius
µL	Microlitre
mL	Millilitre
mM	Millimolar
µM	Micromolar
M	Molar
µg	Microgram
mg	Milligram
rpm	Revolution per minute
nm	Nanometre

CHAPTER I
INTRODUCTION

Life on earth depends on the uptake of energy. While photosynthetic organisms can directly use the sunlight, all other forms of life obtain their energy from nutrients they take up from the environment. One of the most energy-rich sources of food is starch, a carbohydrate food reserve in plants. Starch is the major source of energy for non-photosynthetic organisms, and composed of amylose and amylopectin. Amylose is a linear polymer consisting of up to 6,000 glucose units with α-1,4-glycosidic bonds and amylopectin consists of short α-1,4-linked linear chains of 10-60 glucose units and α-1,6-linked side chains with 15-45 glucose units.

For humans, animals, fungi and bacteria to degrade starch, a whole range of starch-degrading enzymes with different reaction specificities has evolved in these organisms yielding a wide variety of products (Fig. 1.1). A number of these enzymes find application in the industrial processing of starch, either for modification of starch molecules or the production of specific degradation products. This large and diverse group of starch hydrolytic enzymes has been classified in glycosyl hydrolase family 13, the α-amylase family, and presently covers about twenty different enzyme specificities. These enzymes display specificity for either the α- or β-glycosidic bond, have either a retaining or an inverting mechanism depending on whether they retain or invert the anomeric structure of the substrate, and whose activities classify them as either hydrolases (EC 3.2.1) or transferases (EC 2.4.1) (Janecek, 1997; van der Veen *et al*., 2000a; del Rio *et al*., 1997; Uitdehaag *et al*., 2002).

An especially interesting and unique family 13 enzyme is the cyclodextrin glucanotransferase (CGTase; 1,4-α-D-glucan: 1,4-α-D-glucopyranosyltransferase, EC. 2.4.1.19), first observed to be produced by *Bacillus macerans* and has since been found by a variety of bacteria including:

- aerobic mesophilic bacteria: *Pseudomonas* spp., *B. cereus, B. megaterium, B. ohbensis, B. circulans, Paenibacillus macerans, Klebsiella oxytoca, K. pneumoniae, Micrococcus luteus, Brevibacillus brevis*;

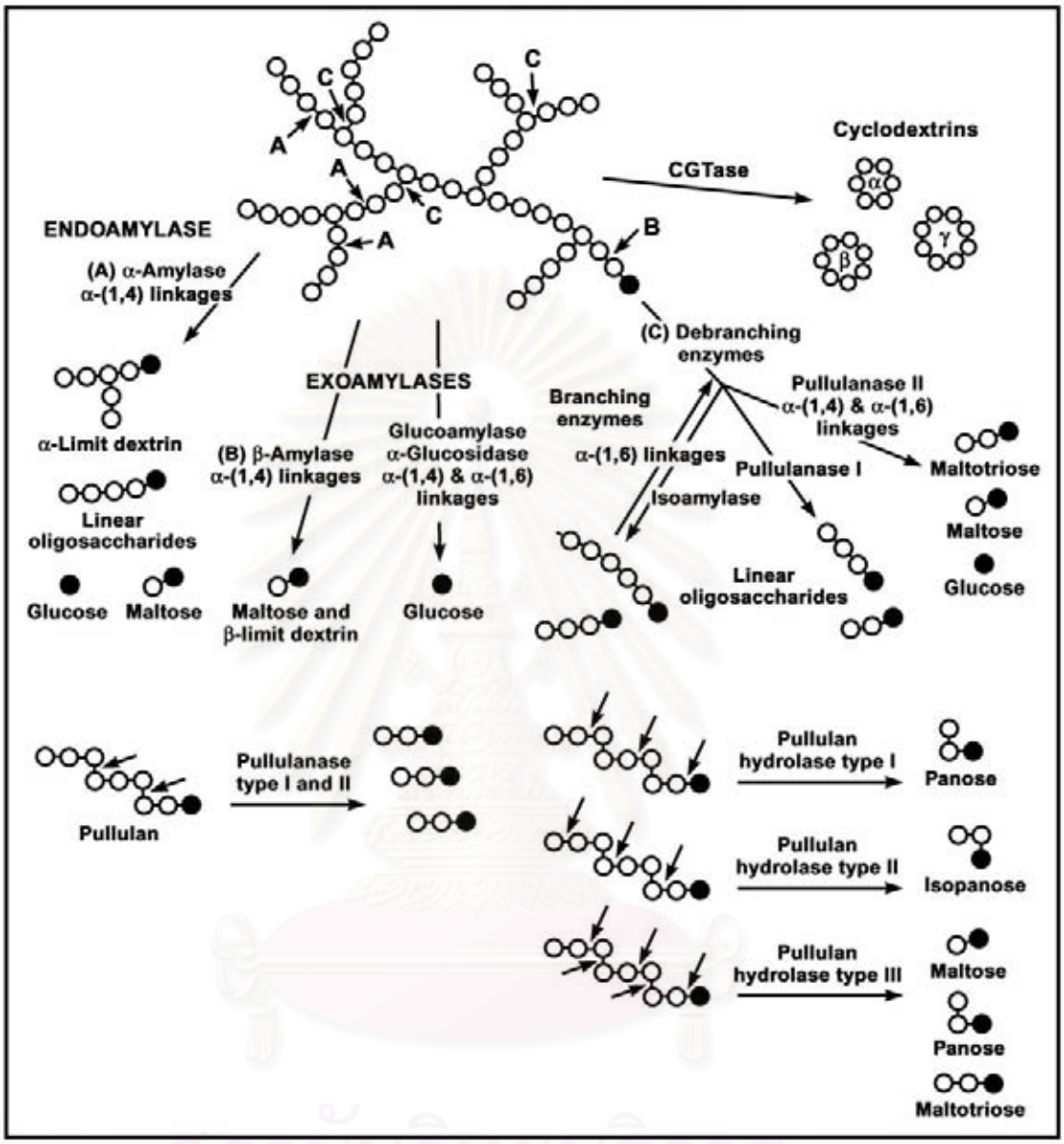

Fig. 1.1. Schematic representation of the action of starch-processing enzymes. (●) glucose molecule with a reducing end; (○) glucose molecule without a reducing end (Bertoldo and Antranikian, 2002; Hobel, 2004).

- aerobic thermophilic bacteria: *B. stearothermophilus*;
- anaerobic thermophilic bacteria: *Thermoanaerobacterium thermosulfunigens*, *Thermoanaerobacter* sp.; and
- aerobic halophilic bacteria: *B. halophilus* (Tonkova, 1998).

When these bacteria excrete CGTases into the starch medium, these CGTases convert starch into cyclodextrins, which are subsequently absorbed and hydrolyzed by another enzyme cyclodextrinase (CDase; cyclomaltodextrin dextrin-hydrolase (decyclizing), EC 3.2.1.54).

There are three major forms of cyclodextrins (CDs), α-, β-, γ-CDs, in the market. In 1970, the price of β-CD was around 2,000 US$/kg, and it was available only as a rare fine chemical, 25 years later, more than half a dozen companies worldwide are producing cyclodextrins. Their total output is in excess of 1,000 tons/year, global consumption was around 6,000 metric tons in 1998 with an annual growth rate of 15-20% and the price of β-CD is lower depending on the quality and delivered quantity. The α- and γ-CDs, as well as several derivatives, (hydroxypropyl-β- and γ-CDs, randomly methylated α- and β-CDs, maltosyl-β-CD, acetylated CDs, etc.) are also produced industrially. The prices of α- and γ-CDs always remain higher than that of the β-CD, partly because of their lower yield (higher solubility), and partly because of the lower volume of their production (Szejtli, 1998; McCoy, 1999). The increasing industrial demand for cyclodextrins is reflected in an increased demand for CGTase preparations. These enzymes are therefore studied extensively, leading to the knowledge of their reaction mechanisms, the factors that determine substrate and product specificity, and the stability of the enzyme.

1.1 Application of cyclodextrins

CGTases are capable of converting starch and related substrates to cyclodextrins. The closed-ring oligosaccharides of the cyclodextrins are joined by α-1,4 glycosidic bond, and mainly consisting of 6, 7 or 8 glucose residues, named as α-, β- and γ-CDs, respectively (Fig. 1.2a). The glucose residues in the cyclodextrin ring are arranged in a manner that the secondary hydroxyl groups at C2 and C3 are located on one edge of the ring and the primary hydroxyl groups (C6) on the other edge. The apolar C3 and C5 hydrogens and the ether-like oxygens are at the inside and the hydroxyl groups at the outside of these molecules. These results in a torus-shaped molecule with a hydrophilic outside, which can dissolve in water, and a hydrophobic cavity, which enables cyclodextrin to form an inclusion with a wide variety of poorly

water soluble compounds, called guest molecules (Fig. 1.2b and 1.2c). The characteristics of the cyclodextrins are summarized in Table 1.1, which provide important parameters for complex formation with hydrophobic compounds or their functional groups (Szejtli, 1998 and van der Veen *et al.*, 2000a).

The formation of inclusion complexes leads to changes in the chemical and physical properties of the encapsulated compounds. This has led to the various applications of cyclodextrins in analytical chemistry, agriculture, pharmaceutical, food, cosmetics, biotechnology and toiletry.

In analytical chemistry, cyclodextrins are used for the separation of enantiomers on HPLC or GC. In nuclear magnetic resonance (NMR) studies, they can act as chiral shift agents and in circular dichroism as selective agents altering the spectra. In electrochemical chemistry, they can be used to mask contaminating compounds, allowing more accurate determinations. In agriculture, cyclodextrins can be applied to delay seed germination, or control of plant growth and to be additives in pesticides. In food industry, cyclodextrins have found several applications such as texture-improvement of pastry and meat products, reduction of bitterness, unwanted tastes and odor, stabilization of flavors and emulsions like mayonnaise, and depletion of cholesterol from milk. In pharmaceutical industry, cyclodextrins increase the water solubility of several poorly water-soluble substances, improve of bioavailability and reduction of side effects, facilitate the handling of volatile products, and reduce the dose of the drug administered. cyclodextrins also improve the stability of substances, *i.e*. increase their resistance to hydrolysis, oxidation, heat, light and metal salts. The inclusions of irritating medicines in cyclodextrins can also protect the gastric mucosa for the oral route, and reduce skin damage for the dermal uses (Penninga, 1996a).

Administered cyclodextrins are quite resistant to starch degrading enzymes, although they can be degraded at very low rates. α-CD is the slowest, and γ-CD is the fastest degradable compound. This is due to their differences in size and flexibility. Degradation is not performed by saliva or pancreatic amylases, but by α-amylases from microorganisms in the colon flora. Absorption studies revealed that only 2-4% of cyclodextrins is absorbed in the small intestines and the remainder is degraded and taken up as glucose. This can explain the low toxicity found upon oral administration of cyclodextrins (Bar and Ulitzur, 1994; Duchene, 1998).

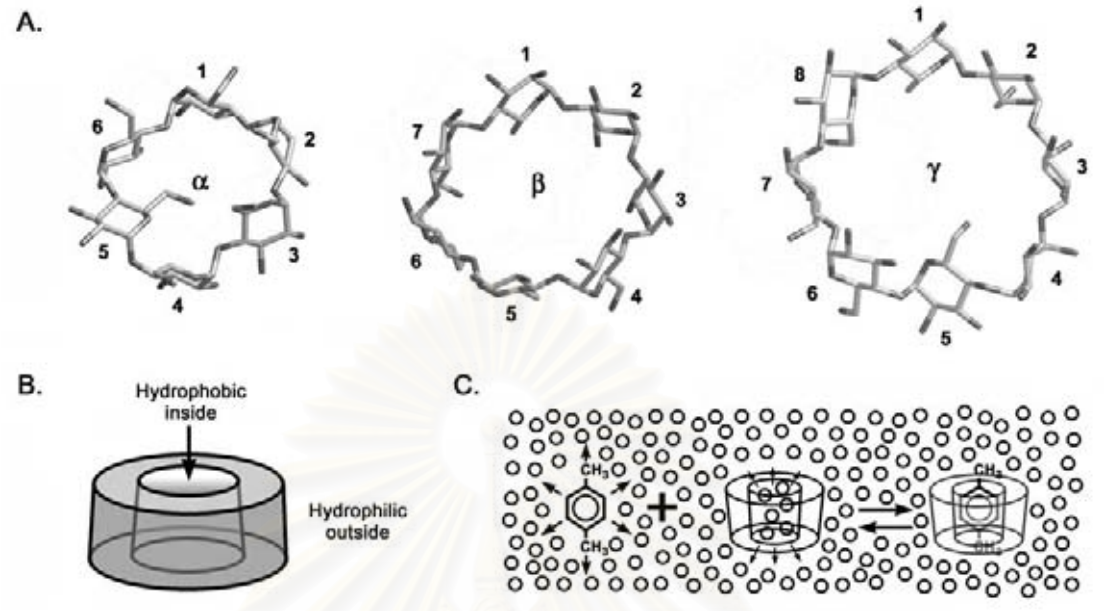

Fig. 1.2. Structures and properties of cyclodextrins. A. the α-, β- and γ-CDs; B. the three-dimensional model and property of cyclodextrin; C. the formation of the inclusion complex of a cyclodextrin with a guest molecule. *p*-Xylene is the guest molecule and the small circles represent the water molecules (Szejtli, 1998 and van der Veen et al., 2000a).

Table 1.1. Characteristics of α-, β-, and γ-CDs (Szejtli, 1988).

Cyclodextrin	α	β	γ
Number of glucose units	6	7	8
Molecular weight (g/mol)	972	1135	1297
Solubility in water, g 100 mL^{-1} at room temp.	14.5	1.85	23.2
Cavity diameter, Å	4.7-5.3	3 6.0-6.5	7.5-8.3
Height of torus, Å	7.9 ± 0.1	7.9 ± 0.1	7.9 ± 0.1
Approx volume of cavity, Å	174	262	427
Crystal forms (from water)	hexagonal plates	monoclinic parallelograms	quadratic prisms

1.2 Commercial production of cyclodextrins using CGTases

In general, the CGTase from *Bacillus macerans* which is used for cyclodextrin production in an industrial scale (Riisgaard, 1991), is poorly active on native starch because of the well-organized structure of the granules held together by internal

hydrogen bonds. The process must run at two different temperatures. In the initial step, liquefied by heat-stable α-amylase treatment at 105 ºC is needed to weaken the hydrogen bonds away from starch molecule. After liquefaction, the starch solution is cooled down to make it suitable for incubation at lower temperature (55 ºC) required for the CGTase catalyzed production of cyclodextrins. However, this procedure is inefficient in many aspects: first, the α-amylase should be inactivated before the addition of CGTase; second, microbial contamination is possible; third, it is time consuming (Chung, 1998) and last, the α-amylase used for liquefaction produces maltodextrins, which can act as acceptor molecules in the coupling reaction of the CGTase, severely reduces the yield of cyclodextrins (Biwer *et al*., 2002). Thus, the use of thermostable CGTase will allow the liquefaction and cyclization to take place in one step for efficient production of cyclodextrins (Niehaus, 1999).

Furthermore, the other disadvantage of cyclodextrin production by CGTase is that all known CGTase enzymes produce a mixture of α-, β- and γ-CDs at different ratios. The isolation of pure cyclodextrins from this mixture requires a series of additional steps, including precipitation with organic solvents that are potentially hazardous to human consumption. A CGTase, which produces only a single type of cyclodextrin, is therefore of high industrial interest (van der Veen *et al.*, 2000a).

1.3 Three-dimensional structure of CGTase

Primary and three-dimensional structural comparisons between CGTases and α-amylases have revealed both common and distinct features among the enzymes. Both CGTases and α-amylases share three structural domains: A, B and C (Rashid, *et al*., 2002) (Fig. 1.3 and 1.4). Domain A comprises 300-400 amino acid residues and contains a highly symmetrical fold of eight parallel β-strands arranged in a barrel encircled by eight α-helices. This $(\beta/\alpha)_8$ or TIM barrel catalytic domain (Fig. 1.3) is present in all enzymes of the α-amylase family. Several proline and glycine residues flanking the loops connecting the β-strands and α-helices are highly conserved in these enzymes (Janecek, 1997; Janecek and Sevcik 1999). The catalytic residues, Glu257, Asp229 and Asp328 (*B. circulans* 251 CGTase numbering), and substrate binding residues are located in the loops at the C-termini of β-strands in domain A.

Moreover, on the basis of the results from many studies on X-ray crystallographic structures of CGTases with their inhibitors, substrates or products, it has been proposed that the active center of CGTase has a tandem subsite architecture in the substrate binding groove, and that it comprises at least nine sugar-binding subsites, designated from the nonreducing end to the reducing end as -7 to +2 (Fig. 1.5) (van der Veen *et al*., 2000a and Strokopytov *et al*., 1996).

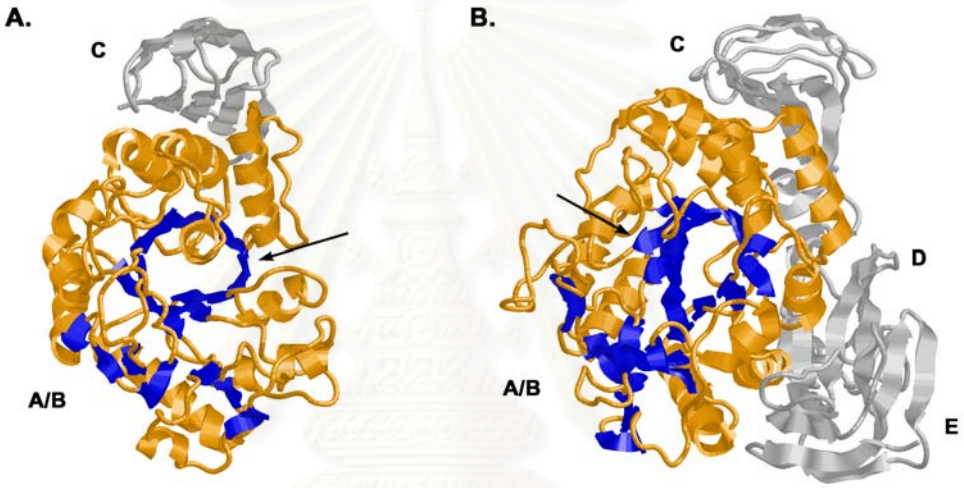

Fig. 1.3. Comparison of the three dimensional structures of α-amylase and CGTase. A, α-amylase from *Bacillus subtilis* (PDB 1BAG; Fujimoto *et al.*, 1998); B, CGTase from *Bacillus circulans* strain 251 (PDB 1CDG; Lawson *et al.*, 1994). Arrows indicate the TIM barrels.

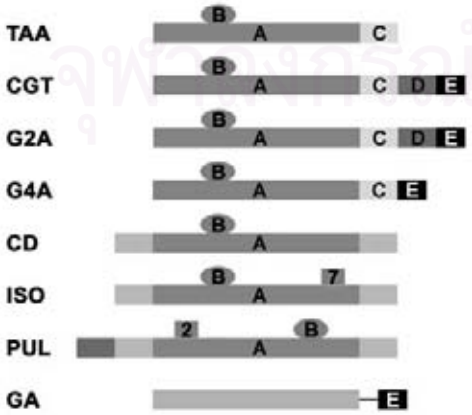

Fig. 1.4. Domain level organization of starch-degradating enzymes. CGT, CGTase from *B. circulans*; G2A, maltogenic α-amylase from *Bacillus stearothermophilus*; G4A, maltotetraose forming α-amylase from *Pseudomonas stutzeri*; TAA, α-amylase from *A. oryzae* (Taka-amylase A); CD, cyclodextrinase from *Klebsiella oxytoca*; ISO, isoamylase from *P. amyloderamosa*; PUL, pullulanase from *K. aerogenes*; GA, glucoamylase (family 15 of glycosyl hydrolases) from *Aspergillus niger*. (van der Veen *et al*., 2000a).

Domain B is an extended loop region inserted between β-strand 3 and α-helix strand 3 of domain A. It is somewhat large, and regarded as a separate structural domain. This domain B consists of 44-133 amino acid residues and contributes to substrate binding by providing several amino acid side chain alongside a long groove on the surface of the enzyme that interact with the substrate (Uitdehaag *et al.*, 2002). Domain C is approximately 100 amino acids long and has an antiparallel β-sandwich fold. The domain C of the CGTase from *B. circulans* strain 251 contains one of the three-maltose binding sites (Lawson *et al.*, 1994) observed from the maltose dependent crystals. This maltose binding site is found to be involved in raw starch binding (Penninga *et al.*, 1996b), suggesting a role of domain C in substrate binding. Others suggest that this domain is involved in bond specificity, particularly in enzymes hydrolyzing or forming the α-(1,6) bonds, e.g., pullulanase, isoamylase and branching enzymes.

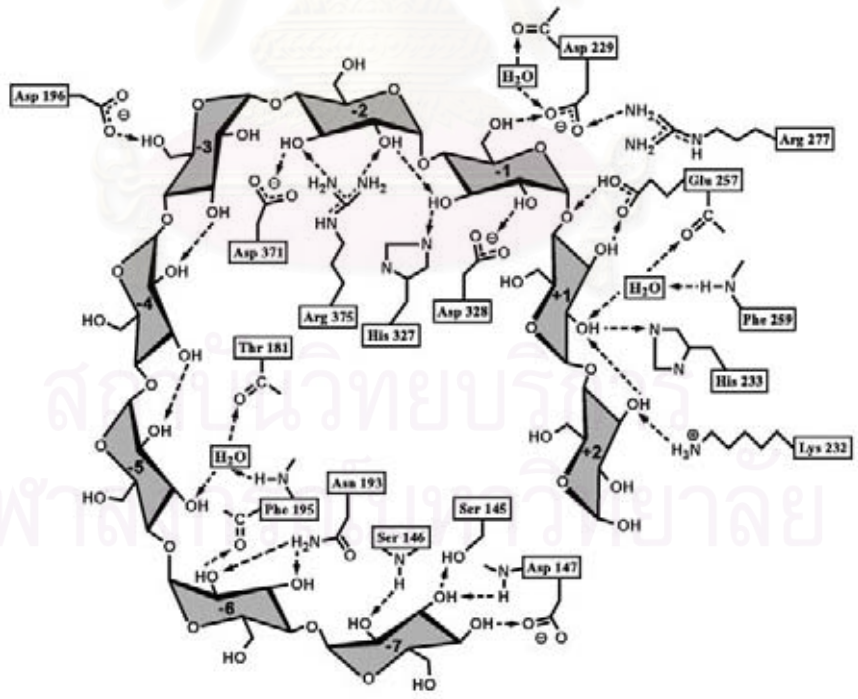

Fig. 1.5. Schematic representation of the hydrogen bonds between the *B. circulans* strain 251 CGTase and a maltononaose inhibitor bound at each subsite of the active site (Strokopytov *et al.*, 1996).

CGTases have two additional domains not found in α-amylases, domains D and E, which have the β-sheet structure (Fig. 1.3). The domain D, consisting of approximately 90 amino acids with an immunoglobulin fold, is almost exclusively found in CGTases and its function is unknown. The domain E consists of approximately 110 amino acids and is found to be responsible for substrate binding. Two maltose-binding sites have been identified in the domain E of CGTase from *B. circulans* 251, and evidence that this domain contributes to raw-starch binding has also been obtained from other CGTases (Svensson *et al.*, 1989).

1.4 CGTase reaction and its catalytic mechanism

The CGTase catalyzes four distinctly different reactions, depending on the nature of the acceptor molecule: three transglycosylation reactions (disproportionation, cyclization and coupling) and a hydrolysis reaction (Fig. 1.6).

i) Disproportionation is an intermolecular transglycosylation reaction. In this reaction a linear malto-oligosaccharide is cleaved and one of the products is transferred to another linear acceptor substrate. This reaction yields a mixture of smaller and longer oligosaccharides.

ii) Cyclization is an intramolecular transglycosylation reaction, in which the non-reducing end of the same oligosaccharide is transferred to the reducing end of the same oligosaccharide chain. The products of this reaction are cyclodextrins.

iii) Coupling is the reverse of the cyclization reaction in which the opening of a cyclodextrin ring is followed by the transferring of the oligosaccharide to a linear saccharide acceptor. This reaction produces a longer chain oligosaccharide.

iv) Hydrolysis is a reaction in which part of a linear oligosaccharide is transferred to water. This reaction is much weaker than the transglycosylation reactions.

Like the α-amylase family, CGTase has the catalytic mechanism as the α-retaining double displacement mechanism. This mechanism involves two catalytic residues, an acid/base catalyst (Glu257 in CGTase) and a nucleophile (Asp229) (Fig. 1.7). When substrate has bound, Glu 257 (as acid) donates a proton to the scissile glycosidic bond oxygen The scissile bond between subsite +1 and -1 is then cleaved,

during which reaction the -1 sugar goes through an oxocarbonium ion-like transition state. In the subsequent reaction step, this oxocarbonium ion-like transition state collapse into a stable covalent glycosyl enzyme reaction intermediate which is β-glycosidically linked to the nucleophile Asp229. The leaving group (at subsite +1) is exchanged for a new compound, the acceptor, which gets activated by Glu257 (now a base). This activated acceptor attacks the covalent intermediate, and via another oxocarbonium ion-like transition state, the final α-1,4 glycosidic product bond is formed (Uitdehaag *et al.*, 2002). However, there is Asp328, catalytic residue, stabilizes the substrate binding and elevates the pK_a of Glu257 that exists only when no substrate or inhibitor is present (Knegtel *et al.*, 1995).

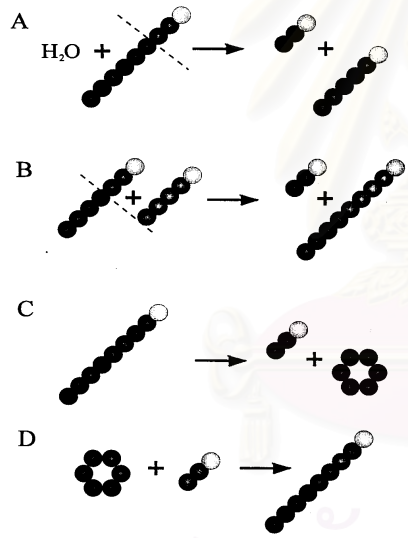

Fig. 1.6. Schematic representation of the CGTase-catalysed reactions. The circles represent glucose residues; the white circles indicate the reducing end sugars. (A) hydrolysis; (B) disproportionation; (C) cyclization; (D) coupling (van der Veen *et al.*, 2000a).

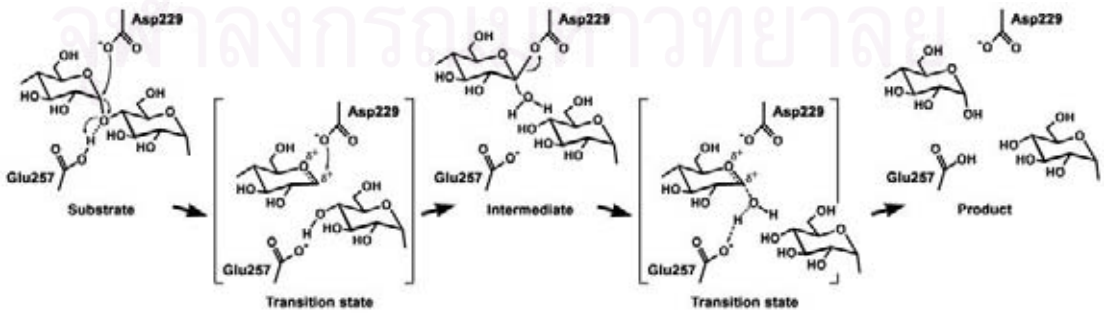

Fig. 1.7. The CGTase reaction mechanism (Uitdehaag *et al.*, 1999 and 2002).

1.5 Thermostability of CGTases

Understanding the molecular basis of protein thermal stability is an important fundamental problem with obvious practical applications. One approach to this problem involves the comparison of structures and sequences of protein from mesophilic and thermophilic organisms (Chakravarty and Varadarajan, 2000) which could provide the important clues to themostability of proteins.

In general, CGTases from many microorganisms have optimum temperature in the range of 40-60 ºC. In contrast, the thermophilic enzymes produced from some anaerobic and aerobic thermophilic bacteria were characterized with high thermostability and a temperature optimum in the range of 80-90 ºC (Table 1.2) (Tonkova, 1998). In the thermostable CGTases which are functional in extreme thermal environment, the NH_2-terminal and the COOH-terminal domains seem to be suitably arranged for efficient cyclodextrin production (Yamamoto, 1999) and only NH_2-terminal of the enzyme was important for heat stability (Kaneko, 1989).

Table 1.2. Some characteristics of the mesophilic and thermophilic CGTases.

Microorganism	Optimum Temp. (ºC)	Product	References
Bacillus circulans 8	ND	β-CD	Nitschke *et al*., 1990
Bacillus circulans 251	ND	β-CD	Lawson *et al.*, 1994
Bacillus stearothermophilus NO2	80	α/β-CD	Fujiwara, 1992
Bacillus stearothermophilus ET1	80	β-CD	Chung, 1998
Thermoanaerobacterium thermosilfurigenes EM1	80-85	β-CD	Wind, 1995
Thermoanaerobacter sp. ATCC 53627	90	α/β-CD	van der Veen *et al.*, 2000a

The availability of the crystal structures at 2.0 Å resolution of the CGTases of the mesophilic *B. circulans* 251 (PDB 1CGD) (Lawson *et al*., 1994) and *B. circulans* 8 (PDB 1CGT) (Klein and Schulz, 1991) (Fig. 1.8), at 2.5 Å resolution of the thermophilic *B. stearothermophilus* (PDB 1CYG) (Kubota *et al*., 1991) and at 2.3 Å of the *Thermoanaerobacterium thermosilfurigenes* EM1 (PDB 1CIU) (Knegtel *et al*., 1996) (Fig. 1.9) allows for detailed amino acid sequence and structural comparison

between the mesophilic and thermostable CGTase molecules. Significant differences are observed in a few regions particularly at the loop regions near the active site (Fig. 1.10). The amino acid residues in these regions possibly contribute with hydrogen bonds and apolar contacts to the stabilization of the thermostable enzyme.

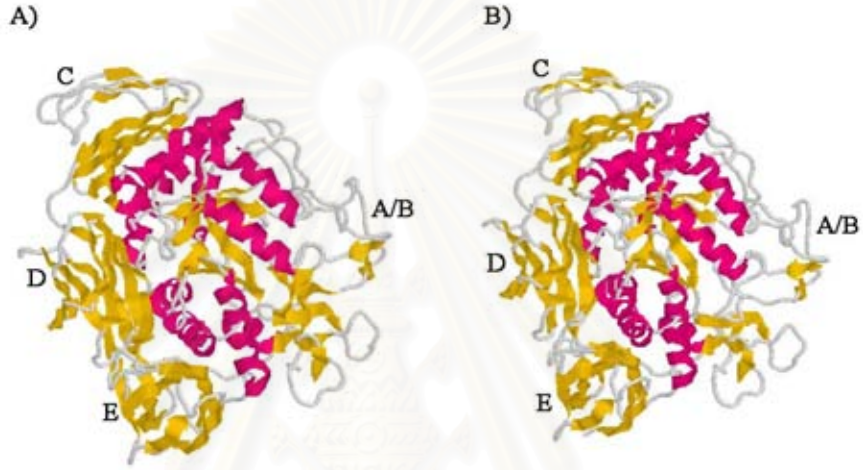

Fig. 1.8. The three dimensional structures of two mesophilic CGTases. A. the mesophilic *B. circulans* 251 (PDB 1CDG), and B. the *B. circulans* 8 (PDB 1CGT).

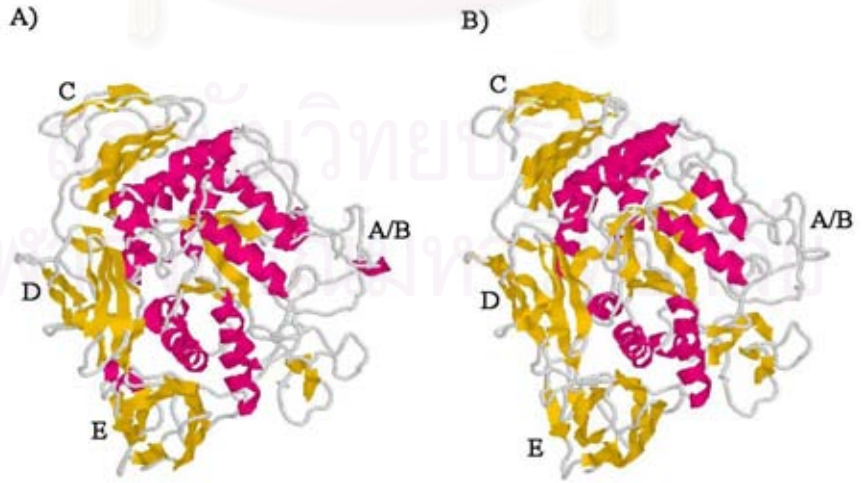

Fig. 1.9. The three dimensional structures of two thermostable CGTases. (A), *Thermoanaerobacterium thermosilfurigenes* EM1 (PDB 1CIU) and (B), *Bacillus stearothermophilus* (PDB 1CYG).

Fig. 1.10. Alignment of amino acid sequences of mesophilic and thermophilic CGTases. BC251, *B. circulans* 251 (PDB 1CDG); BC8, *B. circulans* 8 (PDB 1CGT); TthEM1, *Thermoanaerobacterium thermosilfurigenes* EM1 (PDB 1CIU) and BST2, *B. stearothermophilus* (PDB 1CYG).

Recently, the structural studies of thermophilic enzymes have suggested that an increase in surface salt-bridge could be responsible for structural stability of proteins at elevated temperatures (Chan *et al*., 1995 and Day *et al*., 1992). The mesophilic CGTases from *B. circulans* 251 and *B. circulans* 8 have a total of 27 and 16 salt-bridges, respectively (using a 3.5 Å distance limit for the Arg, Lys, Asp, and Glu charged side-chain atoms), while the *T. thermosilfurigenes* EM1 CGTase has 20. By comparing the location of salt-bridges, Leemhuis *et al*. (2004) indicated that certain salt-bridges were absent in CGTase from *B. circulans* 251 and carried out a mutagenesis experiment to create the salt-bridge. They found that one of the mutant had slightly increased thermostability. The fact that CGTase from *B. circulans* 251 has more salt-bridge than that from *T. thermosilfurigenes* EM1 and the creation of salt-bridge in CGTase has little effect on thermostability indicates that salt-bridge alone is not the major determinant for thermostability.

1.6 Protein engineering for CGTase thermostability

Engineering proteins for thermostability has been vigorously studied in the biotechnical research areas because of the useful application in the industrial scale. Proteins from thermophilic organisms offer good model systems with which to address the origins of thermostability (Strop and Mayo, 2000). Several reasons have been attributed to the greater stability of the thermophilic proteins. Among the most prominent ones are greater core hydrophobicity, deletion or shortening of loops, better packing, smaller and less numerous cavities, increased surface area buried upon oligomerization, amino acid substitutions within and outside the secondary structures, increased occurrence of proline residues, decreased occurrence of thermolabile residues, increased helical content, increased polar surface area, increased hydrogen bonding and salt bridges (Kumar *et al*., 2000).

Protein engineering, usually perform through site-directed mutagenesis is the favorite mode for experimental analysis and stability enhancement. There are many site-directed mutagenesis protocols, which change nucleotide sequence by using specific primer introduced into the part of the interested gene. For CGTases, there are numerous studies to investigate the product specificity of the enzymes while only a

few studies are on the thermostability of CGTase. Thus far, there has been no success in crating the thermostable CGTase from the mesophilic one.

1.7 Scope of this study

As mentioned above, thermostable CGTases are beneficial for the production of cyclodextrins. Several attempts have been made to enhance the stability of CGTases. There are two possible ways to obtain the thermostable CGTases. The first one is the screening for thermophilic microorganisms that produce the thermostable enzymes. The second is to mutagenize the existing CGTase to crate an enzyme with higher thermostability. In this research, the second approach is used. The CGTase gene from *B. circulans* A11 (Rimphanitchayakit *et al*., 2005) is used. The gene encodes a mesophilic β-CGTase of 713 amino acid residues, including a signal peptide. The molecular weight is approximately 72 kDa. The optimal temperature for cyclodextrin production is 60-65 ºC. The changes in product specificity of this enzyme have been studied (Rimphanitchayakit *et al*., 2005; Kerdsin, 2003; Chotechuang, 2003). To create the thermostable version of the CGTase from *B. circulans* A11, the basic differences in the amino acid sequence from the thermostable enzymes are studied. The locations of the amino acid sequence differences on the three-dimensional structure are taken into consideration. Mutagenesis of the CGTase is carried out using the unique site elimination (USE) mutagenesis. The activity of the mutant CGTases under various temperatures is reported.

CHAPTER II
MATERIALS AND METHODS

2.1 Equipments

Autoclave: Model HA-30, Hirayama Manufacturing Corporation, Japan.

Autopipette: Pipetman, Gilson, France.

Balance: Sartorius LC 620, Germany.

Centrifuge: Refrigerated centrifuge: Model J-21C, Beckman Instrument Inc., USA.

Centrifuge: Microcentrifuge High Speed: Model 1110 Mikro 22R, Hettich Zentrifugen, Germany.

Centrifuge: Minimicro DW 41.

Gel document: Syngene, A division of Synoptics Ltd., UK.

Incubator: Heraeus, Germany.

Incubator shaker: Innova 4000, New Brunwick Scientific Co., Inc., USA.

Laminar flow: Issco, USA.

pH meter: Precisa pH900, Precisa instrument AG company, Switzerland.

Freezer: Upright Ultra Freezer; Model MDF-U4086S, Sanyo Electric Trading Co.Ltd., Japan.

Spectrophotometer: Jenway 6400, England.

Vortex: Model 232, Fisher Scientific Inc., USA.

Water bath: MEMMERT GmbH + Co. KG, Germany.

U.V. transilluminator: 2011 MA Crovue, San Gabrial, USA.

Transformation apparatus: Gene Pulser™, Biorad, USA.

High performance liquid chromatography: Shimadzu, Japan.

Power supply: Model EC 135-90, E-C Apparatus Corperation, USA.

2.2 Chemicals

α-, β- and γ-cyclodextrins, Sigma, USA.

Absolute alcohol, Merck, Germany.

Acetonitrile (HPLC grade), Lab Scan, Ireland.

Agar, Merck, Germany.

Agarose, SEAKEM LE Agarose, FMC Bioproducts, USA.

Ampicillin, Biobasic Inc., Thailand.

Boric acid, Merck, Germany.

Bovine serum albumin (BSA), Sigma, USA.

Bromophenol blue, Merck, Germany.

Calcium chloride, Merck, Germany.

Chloroform, Sigma, USA.

Di-Sodium hydrogenphosphate, Fluka, Switzerland.

DNA marker, Lamda (λ) DNA digested with *Hin*dIII: Biobasic Inc., Thailand.

Ethidium bromide, Sigma, USA.

Ethylenediamine tetraacetic acid (EDTA), Fluka, Switzerland.

Glacial acetic acid, BDH, England.

Glucose, Sigma, USA.

Glycerol, Univar, Australia.

Hydrochloric acid, Lab Scan, Ireland.

Iodine, Baker chemical, USA.

Kanamycin, Bio101 Inc., USA.

Methanol, Scharlau, Spain.

NucleoTrap Gel Extraction Kit, BD Biosciences, USA.

Orthophosphoric acid 85%, Carlo Erba, Italy.

Phenol, Pierce, USA.

Polyethylene glycol 6000, Fluka, Switzerland.

Potassium iodide, Mallinckrodt, USA.

QIAprep Spin Miniprep Kit, Qiagen, Germany.

Sodium acetate, Carlo Erba, Italy.

Sodium carbonate, BDH, England.

Sodium chloride, Univar, Australia.

Sodium dihydrogen orthophosphate, Carlo Erba, Italy.

Sodium dodecyl sulfate, Sigma, USA.

Sodium hydroxide, Carlo Erba, Italy.

Soluble starch, Scharlau, Spain.

Tetracyclin, Sigma, USA.

Tris-base, USB, USA.

Tryptone, Merck, Germany.

Yeast extract, Scharlau, Spain.

2.3 Bacterial strains

Escherichia coli JM109 [*F', traD36, proA*$^{+}$*, proB*$^{+}$*, lacI*^{q}*, lacZΔM15/recA1, endA1, gyrA96, thi, hsdR17, supE44, relA1,Δ(lac-proAB), mcrA*] was used for DNA manipulation.

E. coli BMH 71-18 *mutS* [*F', proA*$^{+}$*, proB*$^{+}$*, lacI*^{q}*, lacZΔM15/mutS:Tn10, thi, supE, Δ(lac-proAB*)] was used for mutagenesis.

M13K07 bacteriophage was used for preparing single-stranded DNA.

2.4 Plasmid vector

A plasmid pVR328, a derivative of pUC119 containing the β-CGTase gene from *Bacillus circulans* A11 (Pongsawasdi and Yagisawa, 1987), was used for mutagenesis and constructing the recombinant plasmids containing various combination of mutation regions. Its brief restriction map is shown in Appendix C.

2.5 Enzymes

Restriction endonucleases: *Nde*I, *Nsi*I, *Sph*I, *Hin*dIII, *Sac*II, *Sal*I, and *Bam*HI, were purchased from New England Biolabs Inc.; USA, and *Sca*I was from Fermentas Inc., USA.

T4 DNA ligase and T7 DNA polymerase was purchased from Fermentas Inc., USA.

T4 polynucleotide kinase was purchased from New England Biolabs Inc., USA.

T7 DNA polymerase was purchased from Fermentas Inc., USA.

Amyloglucosidase [(1→4)-α-D-glucohydrolase, EC 3.2.1.3, from *Aspergillus niger*] was purchased from Fluka, Switzerland.

RNase A was purchased from Sigma, USA.

2.6 Media preparation

1. Luria-Bertani broth (LB medium)

LB broth consists of 1% (w/v) Bactotryptone, 0.5% (w/v) yeast extract and 1% (w/v) NaCl, supplemented with 100 μg/mL ampicillin when needed. LB broth was used to cultivate *E. coli* cells.

2. LB-starch agar plate

LB-starch agar consists of 1% (w/v) Bactotryptone, 0.5% (w/v) yeast extract, 1% (w/v) NaCl, 1.6% (w/v) agar and 1% (w/v) soluble starch, supplemented with 100 μg/mL ampicillin when needed. LB-starch agar plate was used for plate-enzyme assays to detect the starch-hydrolyzing activity of CGTase.

2.7 General techniques in genetic engineering

2.7.1 Preparation of competent cells

A single colony of the *E. coli* JM109 or BMH71-18mutS was cultured as a starter in 5 mL of LB medium and incubated at 37 ºC with 250 rpm shaking for 24 hours. The starter was 1:100 diluted in 200 mL of LB-broth in 500 mL Erlenmeyer flask, and the culture was incubated at 37 ºC with 250 rpm shaking until the optical density at 600 nm of the culture reached 0.5-0.6 (~3-4 hours).

The culture was chilled on ice for 15 minutes and the cells were harvested by centrifugation at 6,000 rpm for 15 minutes at 4 ºC. The supernatant was removed. The cell pellet was washed twice with 1 volume and 0.5 volume of cold sterile water, respectively. The cells were resuspended and centrifuged at 6,000 rpm for 15 minutes at 4 ºC. The supernatant was discarded. The pellet was washed with 10 mL of ice cold sterile 10% (v/v) glycerol, and finally resuspended in a final volume of 0.6 mL of ice-cold sterile 10% glycerol. The cell suspension was divided into 40 μL aliquots and stored at –80 ºC until used.

2.7.2 Electroporation

The competent cells were thawed on ice. The cell suspension of 40 μL was mixed with 1-2 μL of the mutagenesis or ligation mixture, mixed well and placed on ice for 1 minute. The mixture was electroporated in a cold 0.2 cm cuvette with the apparatus setting as 2.5 μF, 200 Ω of the pulse controller unit and 2.50 kV.

After one pulse was applied, the cells were resuspended in 1 mL of LB broth and incubated at 37 ºC for 1 hour. The cell suspension was spread on the LB-starch agar plate.

2.7.3 Plasmid preparation (alkaline lysis method)

Cells harboring plasmid were cultured in 1.5 mL LB medium and harvested by centrifugation at 8,000g, 4 ºC for 2 minute. The packed cells were resuspended in 100 μL of solution I (25 mM Tris-HCl, pH 8.0, 10 mM EDTA and 50 mM glucose) by vigorous vortexing. Then 200 μL of solution II (1% SDS, 0.2 N NaOH) was added, mixed by inversion until the mixture was clear. The mixture was neutralized by adding 150 μL of solution III (3 M sodium acetate, pH 4.7), mixed by inversion and kept on ice for 10 minutes. After centrifugation at 10,000g for 10 minutes, 10 mg/mL of RNaseA was added to the supernatant to give a final concentration of 10 μg/mL and incubated at 37 ºC for 20 minutes. The supernatant was extracted with one volume of phenol:chloroform (1:1). Two volumes of absolute alcohol were added, mixed by inversion several times and stored at –20 ºC for 20 minutes. The plasmid was pelleted by centrifugation at 10,000g, washed with 70% ethanol, and vacuum-dried for 10 minutes. The pellet was dissolved in 50 μL TE buffer and stored at –20 ºC.

For DNA sequencing, the QIAprep Spin Miniprep kit was used to prepare the plasmid DNA, and performed according to the kit protocol.

2.7.4 Agarose gel electrophoresis

DNA was analyzed by using 1% agarose gel in TBE buffer (98 mM Tris-HCl, 89 mM boric acid and 2.5 mM EDTA, pH 8.2). DNA samples with 1×tracking dye were loaded into the wells. The gels were run at 100 volts for 1 hour or until bromophenol blue reached the bottom of the gel. After electrophoresis, the gels were stained with 2.5 μg/mL ethidium bromide solution for 2-5 minutes, and the

DNA bands were visualized under the UV light. The sizes of DNA fragments were determined by comparing the relative mobilities with those of standard DNA fragments (λ/*Hin*dIII marker).

2.7.5 Extraction of the DNA fragment from the agarose gel

The Nucleotrap gel extraction kit was used for extracting DNA fragment from the agarose gel, and performed according to the kit protocol. Briefly, a gel piece containing the DNA fragment was excised from an agarose gel. The weigh of the gel slice was measured and transferred to a 1.5 mL microcentrifuge tube. Three volumes of Buffer NT1, and 4 μL of Nucleotrap suspension for each 1 μg of DNA to be purified were added. The mixture was incubated at 50 ºC for 5-15 minutes and vortexed briefly during the incubation time. The sample was centrifuged at 10,000 rpm for 30 seconds at room temperature. The pellet was washed with 500 μL of Buffer NT2 and 500 μL of Buffer NT3, respectively. Finally, the pellet was added Buffer NE to elute DNA by incubating at room temperature for 10-15 minutes and occasional vortexing during the incubation time. The DNA fragment was collected by centrifugation.

2.7.6 Preparation of single-stranded plasmid

Single-stranded plasmid was prepared from pVR328, a pUC119 plasmid carrying the β-CGTase gene from *B. circulans* A11, by using helper phage M13KO7. A single colony of *E. coli* JM109, containing pVR328, was inoculated into LB broth containing ampicillin 100 μg/mL and incubated with shaking at 37 ºC for 2-3 hours or until the cell density was very slightly turbid. Then, the culture was added the helper phage to 10^7-10^8 pfu/mL and grown at 37 ºC for 1-2 hours with vigorous shaking. The culture was added kanamycin to 70 μg/mL to select for the phage-infected cells and further grown at 37 ˚C for 12-18 hours with vigorous shaking. The 1.5 mL of the cell culture was centrifuged for 5 minutes at 10,000g in a microcentrifuge. The supernatant of 1.2 mL was removed to a new tube. The supernatant was added 200 μL of a PEG solution containing 20% PEG8000 and 2.5 M NaCl, mixed, and incubated to allow the phage particles to precipitate on ice for 30 minutes. The mixture was centrifuged for 15 minutes at 10,000 rpm to collect the phage precipitate. The pellet was resuspended in 90 μL of TE buffer and 10 μL of 3

M sodium acetate, pH 5.5. The suspension was extracted with one volume phenol:chloroform (1:1) and one volume chloroform, respectively. Two volumes of absolute alcohol were added, mixed and stored at –20 ºC for 30 minutes. The single-stranded plasmid was pelleted by centrifugation at 10,000 rpm, washed with 70% ethanol and dried. The pellet was dissolved in 30 μL TE buffer.

2.7.7 Phosphorylation of oligonucleotide primers

Two mutagenic oligonucleotides, named A and B, were purchased from Biobasic Inc., Thailand, and the other two mutagenic oligonucleotides, named C and D, were purchased from Proligo Singapore Pty Ltd, Singapore. They were phosphorylated before use in the mutagenesis procedure. Approximately 100-200 pmol of an oligonucleotide was kinased in 10 μL reaction containing 1× kinase buffer, 1 mM ATP, and 10 U T4 kinase, and incubated at 37 ºC for 1 hour. The reaction was stopped by heating at 70 ºC for 15 minutes. Then, the reaction was spun for 1 minute and stored at –20 ºC.

2.8 Mutagenesis of β-CGTase gene using the USE (Unique Site Elimination) procedure

The four mutagenic primers, A, B, C and D, were designed according to the amino acid regions of β-CGTase that were different from those of other thermostable CGTases. The nucleotide sequences of the four primers are shown in Fig. 2.1 For the screening of the mutants, primers A, B, C, and D were also designed to contain the *Bam*HI, *Sal*I, *Sal*I, and *Hin*dIII, respectively.

The USE mutagenesis procedure is summarized in Fig. 2.2. The procedure works by simultaneously annealing two oligonucleotides primers to a single-stranded plasmid. One primer introduces the desired mutation, and the other primer mutates a restriction site unique to the plasmid for the purpose of selection. The selection primer, called *Sca*I primer, eliminates the *Sca*I site at the ampicillin resistant gene in the plasmid. Each of the four kinased mutagenic primers, the kinased *Sca*I primer and 40 ng of the single-stranded plasmid were mixed in 10 μL reaction containing annealing buffer (200 mM of Tris-HCl, 100 mM of $MgCl_2$ and 500 mM NaCl). The reaction mixture was heated at 95 ºC for 5 minutes, and then placed at room

temperature for 15 minutes. Next, it was added 6 μL of an enzyme mixture containing 1× polymerase buffer, 1 U T7 polymerase, 5 U T4 ligase, 2.5 mM dNTPs, and 10 mM ATP. It was incubated at 37 ºC for 1-2 hours. The reaction mixture was then transformed into an *E. coli* strain BMH71-18*mut*S. A mixture of plasmids were generated by culturing the transformation mixture in the presence of 100 μg/mL ampicillin overnight, pelleting the cells and preparing the plasmids. The plasmid mixture was digested with *Sca*I to linearize most of the wild-type plasmid, and transformed into an *E. coli* strain JM109 to separate individual clones. Colonies were cultured for plasmid miniprep and screened for the plasmids with the added restriction sites by using restriction enzyme digestion.

PRIMER A (47mer)

*Bam*H I

5′ C GTG ATA AGC CGT GGA TCC GCC GAA GGT GGA ATC GTT GAT CAC GCT G 3′

PRIMER B (41mer)

Sal I

5′ C GTG ATA AGC CGT CGA CCC GCT GGC ATC GTT GAT CAC GCT G 3′

PRIMER C (51mer)

Sal I

5′ GGA CTC GTT AGC GAA GTA ATG ATT GTT CGG GTC GAC CTC ATT GAC GCC AAG 3′

PRIMER D (56mer)

*Hin*d III

5′ C CAG CGC CTG CTC AAG CTT CCG TG$^{T}/_{G}$ GTC GCC CTC G$^{C}/_{T}$C G$^{T}/_{A}$T GTA GAA ACG CTC CAT G 3′

Fig. 2.1. The mutageneic oligonucleotides used to produce the mutations in the USE mutagenesis procedure. The restriction recognition sites, which allow rapid screening of the potential mutants, are shaded.

The mutation regions were confirmed using DNA sequencing service by Bioservice unit, National Center for Genetic Engineering and Biotechnology (BIOTEC). The correctness of DNA sequences around the mutation regions was also determined. The DNA sequences were subcloned into the same location in the original plasmid (pVR328) to avoid possible other mutated sequenced in the mutated plasmids.

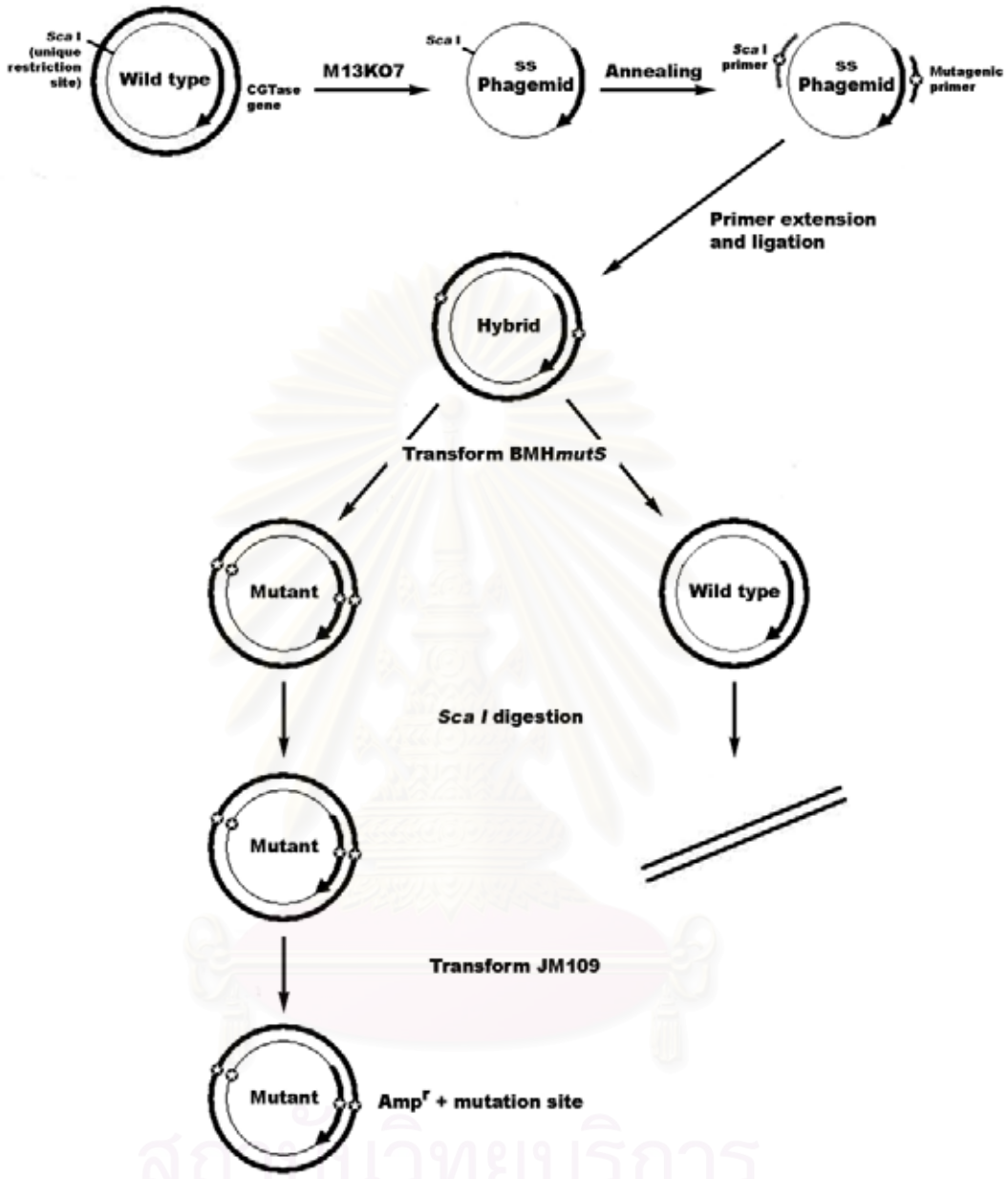

Fig. 2.2. Schematic diagram of USE mutagenesis protocol.

2.9 Construction of the recombinant plasmids containing various combination of the mutant regions

The mutated regions in the mutated plasmids were subcloned into the same regions in pVR328. The plasmids were digested with the appropriate restriction

enzymes to yield DNA fragments containing the mutant regions. The DNA fragments were gel purified using agarose gel electrophoresis and eluted with Qiaquick gel extraction kit. The eluted fragments from mutant plasmids and the restriction enzyme-digested pVR328 were mixed and ligated with T4 DNA ligase. The ligation reactions were incubated for 16-24 hours at 22 ºC. The ligation mixture was used to transform the *E. coli* JM109 by electroporation. The transformants were plated on the LB agar containing 100 μg/mL of ampicillin at 37 ºC for an overnight. Each transformant was grown in the LB broth in the presence of 100 μg/mL ampicillin. In order to verify the presence of the mutation, the recombinant plasmids were screened for the mutant regions by restriction enzyme digestion. They were checked for the cloning sites as well. The recombinant plasmids were constructed such that they contained all possible combinations of the mutant regions.

2.10 Detection of the mutant CGTase activity

2.10.1 Dextrinizing activity

1. Halo zone on LB-starch agar

E. coli JM109 cells, containing a CGTase plasmid, were plated on a LB-starch agar plate and incubated at 37 ºC for 48 hours. The halo formation was observed after the iodine solution (0.02% (w/v) I_2 in 0.27% (w/v) KI) was poured onto the agar.

2. Dextrinizing activity assay

The *E. coli* JM109 cells, containing the CGTase plasmid, were grown at 37 ºC for 16 hours in LB broth containing ampicillin. The culture was centrifuged to remove the cells, and the supernatant liquid was used as crude enzyme preparation.

CGTase activity was measured as the dextrinizing power according to the method of Fuwa (1954) with slight modification. The reaction mixture was performed by pre-heating the 500 μL of 0.2% soluble starch in 0.2 M phosphate buffer, pH 6.0, at each temperature (40, 50, 60, 65, 70, and 80 ºC) for 1 minute. Then 100 μL of appropriately diluted (1:10-1:50) enzyme solution was added and incubated

at that temperature for 10 minutes. To stop the enzymatic reaction, 1 mL of 0.2 N HCl was added to the reaction mixture. The iodine-starch complex (blue color) was developed by mixing 400 μL of the reaction mixture with 4 mL of 0.01% (w/v) I_2 in 0.1% (w/v) KI. The solution was placed at room temperature for 20 minutes, and the absorbance at 600 nm was measured. The experiments were done in duplicate at each temperature. The results were expressed as the mean values of the duplicate experiments.

One unit of enzyme is defined as the amount of enzyme, which produces 10% reduction in the intensity of the blue color of the starch-iodine complex per minute under the described condition. The relative activity was calculated by using a no enzyme control with the highest absorbance as 0%, and zero absorbance as 100%.

2.10.2 CGTase thermostability testing

The thermostability was determined according to the method of Lemmhuis *et al*. (2003) with slight modification. Appropriately diluted crude enzyme of 100 μL was incubated for 10 minutes at various temperatures (40, 50, 60, 65, 70, and 80 ºC), and placed at 40 ºC for 1 minute. Then, 500 μL of 0.2% soluble starch in 0.2 M phosphate buffer, pH 6.0, pre-incubated at 40 ºC were added and further incubated for 10 minutes. The enzymatic reaction was stopped by adding 1 mL of 0.2 N HCl.. The iodine-starch complex (blue color) was developed by mixing 400 μL of the reaction mixture with 4 mL of 0.01% (w/v) I_2 in 0.1% (w/v) KI. The solution was placed at room temperature for 20 minutes, and the absorbance at 600 nm was measured. Duplicate experiments were done at each temperature. The results were expressed as the mean values of the duplicate experiments.

2.10.3 Cyclodextrin-forming activity

The crude enzyme preparations were diluted with 0.2 M phosphate buffer, pH 6, such that the concentrations of the protein were 80 μg/mL. Then, 200 μL of the diluted enzyme preparation from each mutant plasmid was incubated with 0.5 mL of 1% soluble starch at 37 ºC for 12 hours. The reaction was stopped by boiling for 10 minutes, and clarified by centrifugation. The mixture was treated further for four hours with 6U of glucoamylase to digest the remaining starch and

oligosaccharides formed from CGTase reaction. The glucoamylase reaction was stopped by boiling for 10 minutes, and clarified by centrifugation. The cyclodextrin samples were filtered by syringe through the 0.45 μm Sartolon polyamide membrane (Sartorius, Germany) prior to HPLC analysis. The samples were analyzed using the HPLC with a Hypersil-APS2 (NH_2) column (0.46×250 mm), acetonitrile/water (63:37 (v/v)) at flow rate 1.0 mL/min and a refractometric detector. The cyclodextrin standard was a mixture of α-, β- and γ-cyclodextrins (10 mg/mL each). For quantitative analysis, peak area corresponding to each cyclodextrin was used to calculate the cyclodextrin product ratios.

2.11 Protein determination

The protein sample (100 μL) was mixed with 1 mL of Coomassie blue reagent (Appendix A), and left stand at room temperature for 5-10 minutes. The wavelength of 595 nm was measured. The protein concentration was calculated from a standard curve of bovine serum albumin.

CHAPTER III
RESULTS

3.1 Amino acid sequence comparison and the design of mutagenic primers

CGTases from different sources have different characteristics in terms of activity, optimum temperature, thermostability, substrate specificity, and some local structures. The differences lie on the primary amino acid sequence, which dictates the higher-level structure of the enzyme. It is believed that one could simulate one enzyme with the other by mimicking the primary structure of the former enzyme. In this study, I attempted to create a thermophilic CGTase from the mesophilic one from *Bacillus circulans* A11 (A11 CGTase). The amino acid sequences from different thermophilic organisms were downloaded from the GenBank for amino acid sequence comparison. They were CGTases from *Thermoanaerobacterium thermosulfurigenes* EM1 (Tonkova, 1998) *Thermoanaerobacter* sp. ATCC 53627, *B. stearothermophilus* NO2 and *B. stearothermophilus* ET1 (Chung *et al*., 1998), which had temperature optima of 80-85, 90 and 80 ºC, respectively. Of these, the crystal structures of CGTases from *T. thermosulfurigenes* EM1 (Knegtel *et al.*, 1996) and *B. stearothermophilus* (Kubota M, Matsuura Y, Sakai S, Katsube Y, PDB 1CYG, unpublished) were known.

The amino acid sequence of CGTase from *B. circulans* A11 was then compared to those of the thermostable CGTases using clustalX (Thompson *et al*., 1999). The result is shown in Fig. 3.1. The result shows moderate homology (~70%) among the five CGTases as several homologous segments are seen scattering all over the entire amino acid sequences. There are, however, three major and one minor regions in the A11 CGTases that are different from those of thermostable CGTases. The four regions (I, II, III and IV) consist of amino acid residues at positions 89-94, 265-271, 333-339, and 538-540 (A11 CGTase numbering), respectively. The first three regions reside in the catalytic domain A/B while the fourth region is located in domain D whose function is not fully unveiled. The fourth region is likely not

involved in the thermostability of the enzyme since it is found also in some thermostable CGTases.

The primers, corresponding to the three different amino acid regions in A11 CGTase, were then designed. The designed primers mimic the amino acid residues of the thermostable CGTases. Two primers, A and B, were designed for region I mutagenesis, because there were variation in amino acid sequences among the four thermostable CGTases. Primers C and D were designed for region II and III mutagenesis, respectively. Primer A and B introduced the base substitutions/addition and substitutions/deletion, respectively. Primer C and D provided only base substitutions (Fig. 3.2). Amino acid substitutions were made in favor of the amino acid sequence in CGTase from thermostable enzyme. Upon mutagenesis, the amino acid sequences in CGTase from *B. circulans* A11 would be changed to DSTFGGS, DASGS, VDPNNHY, and YIGEGDT in regions I_A, I_B, II, and III, respectively. For the screening of mutants, primers A, and D were designed to create restriction sites, *Bam*HI and *Hin*dIII, respectively, in the mutant plasmids. Primers B and C were both designed to create the same restriction site, *Sal*I, in the mutant plasmids.

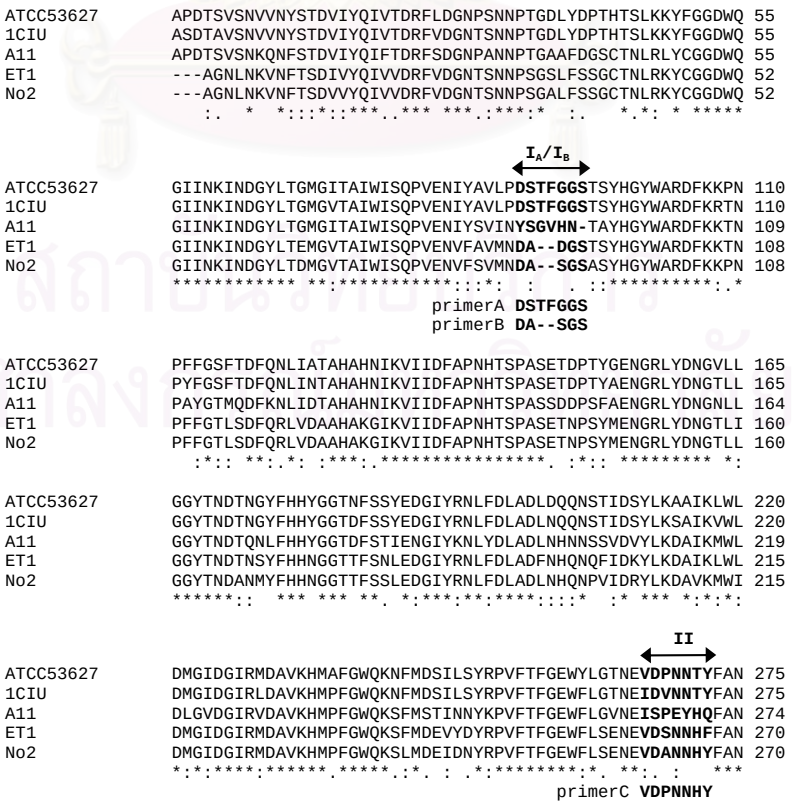

Fig. 3.1. Amino acid sequence comparison of the various CGTases. The different amino acid sequences of CGTases from *Thermoanaerobacterium thermosulfurigenes* EM1 (1CIU), *Thermoanaerobacter* sp. ATCC 53627 (ATCC53627), *Bacillus circulans* A11 (A11), *Bacillus stearothermophilus* NO2 (No2) and *Bacillus stearothermophilus* ET1 (ET1) were aligned. Double arrows indicate the four amino acid sequence regions of the CGTase from *B. circulans* A11 that are different from those of thermostable CGTases. Numbering of the amino acid sequence starts at the N- terminal amino acid of each mature enzyme.

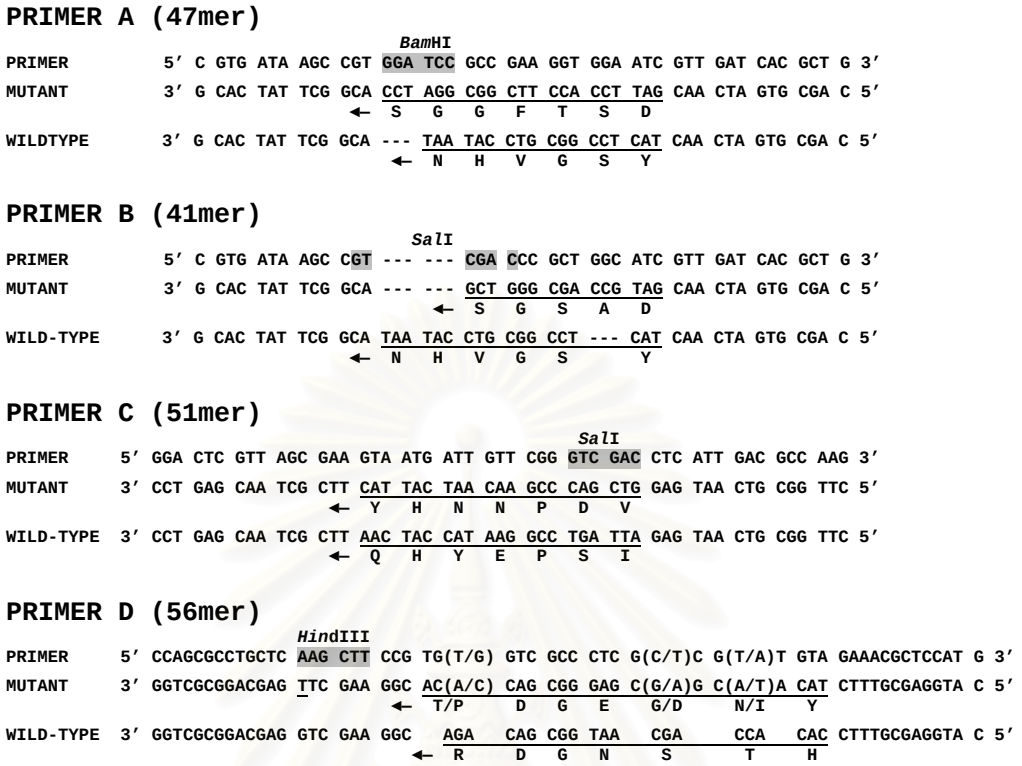

Fig. 3.2. The design of oligonucleotides used in the USE mutagenesis procedure. The nucleotide sequences of wild type to be mutated are underlined. The newly created restriction sites are shaded.

3.2 Mutagenesis of CGTase gene from *Bacillus circulans* A11

The plasmid pVR328, carrying the CGTase gene from *B. circulans* A11, was used as a template for the USE mutagenesis procedure (Fig.2.2). The mutagenic primers A, B, C, and D along with the reference *Sca*I primer were used to mutate the CGTase gene at the three regions described above. The mutagenesis procedure generated a mixture of mutated plasmids. After removing the mostly wild type plasmids with *Sca*I digestion, the mutated plasmids were separated into individual clones by transformation. The plasmid clones were prepared, and screened for the presence of added restriction sites, *Bam*HI, *Sal*I, and *Hin*dIII. The positions of these sites were confirmed by restriction enzyme digestion and agarose gel electrophoresis (Fig. 3.3). Four mutated plasmids, pRS1A, 1B, 2 and 3, were obtained as shown in Fig. 3.4 with the restriction sites, *Bam*HI, *Sal*I, *Sal*I, and *Hin*dIII, respectively. It

should be noted that the pRS3 were obtained after screening nine clones because the designed primer contained multiple nucleotides in several positions in order to create multiple mutated sequences. Two identical clones were selected after restriction digestion and DNA sequencing. Only one clone was chosen to represent the pRS3.

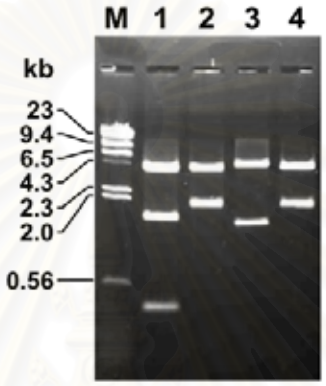

Fig. 3.3. Restriction digestion of pRS1A, 1B, 2, and 3. Lane M: λ/*Hin*dIII marker; lane 1: pRS1A digested with *Bam*HI, lane 2: pRS1B digested with *Sal*I, lane 3: pRS2 digested with *Sal*I, and lane 4: pRS3 digested with *Hin*dIII**.**

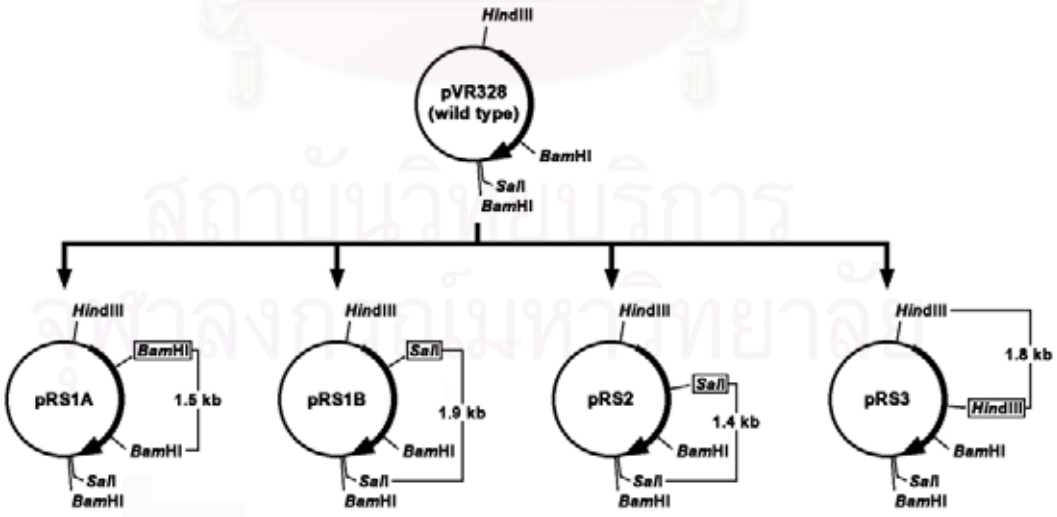

Fig. 3.4. The mutated plasmids, pRS1A, 1B, 2 and 3. The plasmids were processed to confirm the mutations by restriction digestion and DNA sequencing. The new restriction sites are boxed and the sizes of the DNA fragments are indicated.

3.3 DNA sequencing determination of the mutation regions

The precise DNA sequences around the mutation regions in pRS1A, 1B, 2 and 3 were determined using the ABI Prism Big Dye Terminator Cycle Sequencing. The four mutants had the nucleotide sequences as designed (Fig. 3.5). Nucleotide sequences between the two restriction sites bordering the mutation regions were also checked to make certain that there were no additional mutations. The mutation regions were subsequently subcloned using the two border restriction sites into the wild-type plasmid replacing the wild-type sequences.

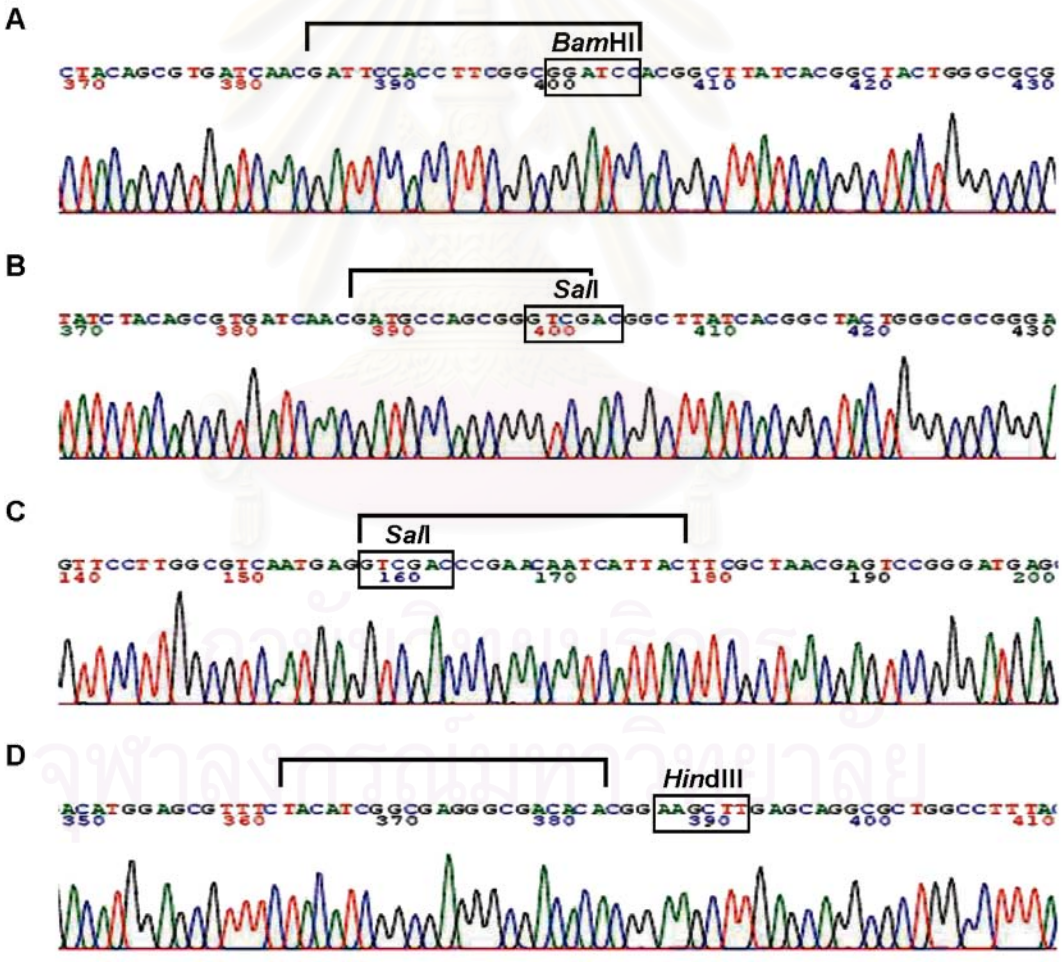

Fig. 3.5. Nucleotide sequencing of mutant regions I_A (A), I_B (B), II (C), and III (D) in pRS1A, 1B, 2 and 3, respectively. The new restriction sites are boxed. Each mutation region is indicated by a line over the region.

3.4 Construction of the mutant CGTases

The DNA fragments containing the mutation regions were subcloned into the original plasmid (pVR328) replacing the wild-type sequence to avoid other possible mutation sequences in the mutated plasmids. Then, the resulting plasmids were used for the construction of mutant CGTases that had the combinations of mutation regions.

To subclone the mutation regions into the pVR328, the DNA fragments between the restriction sites indicated in Fig. 3.6 were removed from pRS1A and 1B as the 608 bp *Nsi*I-*Sph*I fragments, and pRS2 and 3 as the 680 bp *Nde*I-*Sac*II fragments, and replaced the corresponding fragments in pVR328. These resulted in pRS4A, 4B, 5 and 6, respectively. The combination of mutant regions was further constructed. The cloning sites were *Nde*I and *Sac*II, which covered the mutation regions II and III. The pRS7A, 7B, 8A, 8B, 9, 10A and 10B were mutant plasmids containing the mutation regions I_A+II, I_B+II, I_A+III, I_B+III, II+III, I_A+II+III and I_B+II+III, respectively (Fig. 3.6).

The plasmid pRS7A, 7B, 8A and 8B were constructed by subcloning the mutation regions II and III in place of the wild-type sequences in pRS4A and 4B. Thus, the pRS7A contained additional *Bam*HI and *Sal*I sites and the pRS7B contained two additional *Sal*I sites. The pRS8A and the pRS8B contained the additional *Bam*HI and *Hin*dIII sites and the additional *Sal*I and *Hin*dIII sites, respectively.

The pRS9, which contained regions II and III with the additional *Sal*I and *Hin*dIII sites, was constructed by mutating the single-stranded pRS6 DNA with primer C using USE mutagenesis procedure. This was due to the fact that there were no appropriate restriction sites between regions II and III that could be used for cloning. After obtaining the mutant plasmid pRSCD108 with regions II and III mutated and DNA sequencing to confirm the correct mutation, the combination was subcloned into the pVR328 resulting in pRS9. The pRS10A and 10B, which contained all three mutation regions, were constructed by subcloning mutated regions II and III in pRS9 replacing the corresponding sequences in pRS4A and 4B, respectively. The mutated plasmids, pRS10A and 10B, therefore, contained *Bam*HI, *Sal*I and *Hin*dIII sites, and *Sal*I, *Sal*I and *Hin*dIII sites, respectively.

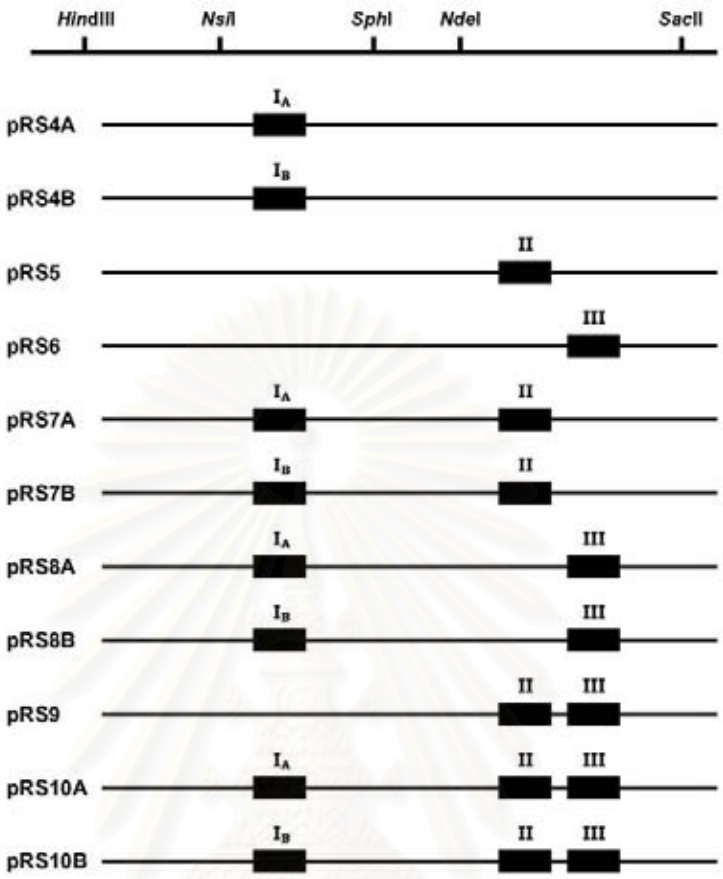

Fig. 3.6. Summary of the mutant CGTase constructs. Regions I_A, I_B, II, and III are the mutated regions containing the restriction sites, *Bam*HI, *Sal*I (for I_B and II) and *Hin*dIII, respectively. The drawing is not to scale.

These recombinant plasmids were subjected to restriction digestion to verify not only the mutation regions but also the cloning sites (Fig. 3.7 and 3.8). The pRS4A was digested with *Bam*HI and *Nsi*I+*Sph*I for the mutation regions and the cloning sites giving 4.3+1.5+0.4 kb and 5.6+0.6 kb DNA fragments, respectively (Fig. 3.7 lanes 1 and 2). The pRS4B was digested with *Sal*I and *Nsi*I+*Sph*I for the mutation regions and the cloning sites giving 4.3+1.9 kb and 5.6+0.6 kb DNA fragments, respectively (Fig. 3.7 lanes 3 and 4). The pRS5, 6, 7A, 7B, 8A, 8B, 9, 10A, and 10B were digested with *Nde*I+*Sac*II for the cloning sites resulting in 5.3+0.9 kb DNA fragments (Fig. 3.7 lanes 6, 8, 10 and 12, and Fig. 3.8 lanes 2, 4, 7, 9 and 12). The pRS5 was digested with *Sal* I for the mutation regions resulting in 4.8+1.4 kb DNA

fragments (Fig. 3.7 lane 5). The pRS6 was digested with *Hin*dIII for the mutation regions resulting in 4.4+1.8 kb DNA fragments (Fig. 3.7 lane 7). The pRS7A was digested with *Bam*HI+*Sal*I for the mutation regions resulting in 4.2+1.1+0.5+0.4 kb DNA fragments (Fig. 3.7 lane 9). The pRS7B was digested with *Sal*I for the mutation regions resulting in 4.3+1.4+0.5 kb DNA fragments (Fig. 3.7 lane 11). The pRS8A was digested with *Bam*HI+*Hin*dIII for the mutation regions resulting in 3.2+1.1+0.8+0.7+0.4 kb DNA fragments (Fig. 3.8 lane 1). The pRS8B was digested with *Sal*I+*Hin*dIII for the mutation regions resulting in 3.2+1.2+1.1+0.7 kb DNA fragments (Fig. 3.8 lane 3). The pRS9 was digested with *Sal*I and *Hin*dIII for the mutation regions resulting in 4.8+1.4 kb and 4.4+1.8 kb DNA fragments, respectively (Fig. 3.8 lanes 5 and 6). The pRS10A was digested with *Bam*HI+*Sal*I+*Hin*dIII for the mutation regions resulting in 3.2+1.1+0.8+0.5+0.4+0.2 kb DNA fragments (Fig. 3.8 lane 8). The pRS10B was digested with *Sal*I and *Bam*HI for the mutation regions resulting in 4.3+1.4+0.5 kb and 4.3+1.9 kb DNA fragments, respectively (Fig. 3.8 lanes 10 and 11).

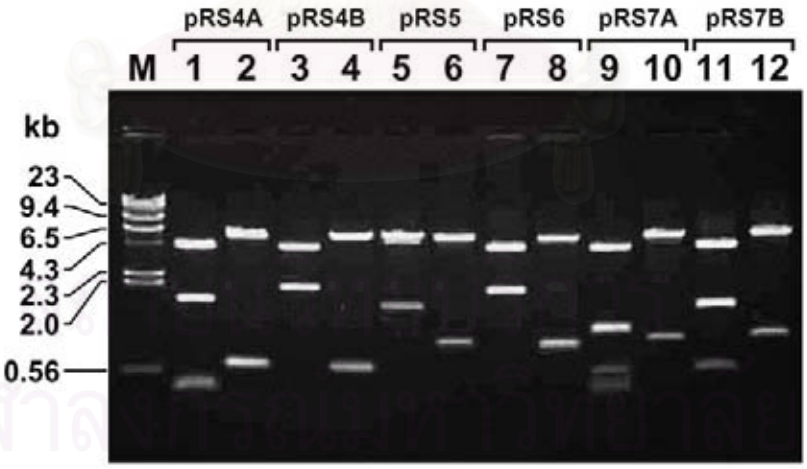

Fig. 3.7. Restriction digestion of pRS4A, 4B, 5, 6, 7A and 7B. Lane M: λ/*Hin*dIII marker; lanes 1 and 2: pRS4A digested with *Bam*HI and *Nsi*I+*Sph*I, respectively; lanes 3 and 4: pRS4B digested with *Sal*I and *Nsi*I+*Sph*I, respectively; lane 5 and 6: pRS5 digested with *Sal*I and *Nde*I+*Sac*II, respectively; lane 7 and 8: pRS6 digested with *Hin*dIII and *Nde*I+*Sac*II, respectively; lane 9 and 10: pRS7A digested with *Bam*HI and *Nde*I+*Sac*II, respectively; lane 11 and 12: pRS7B digested with *Sal*I and and *Nde*I+*Sac*II, respectively.

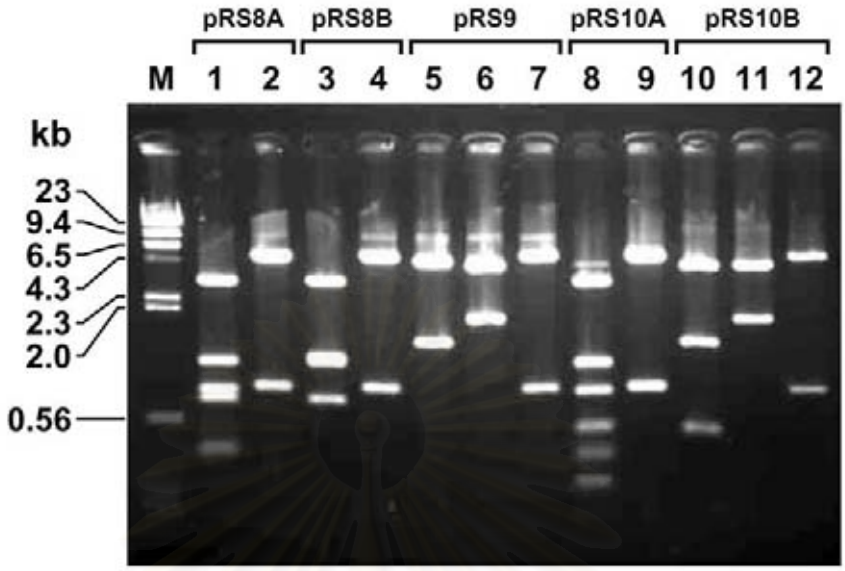

Fig. 3.8. Restriction digestion of pRS8A, 8B, 9, 10A and 10B. Lane M: λ/*Hin*dIII marker; lanes 1 and 2: pRS8A digested with *Bam*HI+*Hin*dIII and *Nde*I+*Sac*II, respectively; lanes 3 and 4: pRS8B digested with *Sal*I+*Hin*dIII and *Nde*I+*Sac*II, respectively; lane 5, 6 and 7: pRS9 digested with *Sal*I and *Hin*dIII and *Nde*I+*Sac*II, respectively; lane 8 and 9: pRS10A digested with *Bam*HI+*Sal*I+*Hin*dIII and *Nde*I+*Sac*II, respectively; lane 10, 11 and 12: pRS10B digested with *Sal*I and *Hin*dIII and *Nde*I+*Sac*II, respectively.

3.5 The activities of the mutant CGTases

3.5.1 Halo zone on LB-starch agar

The *E. coli* JM109 transformants harboring each of the mutant CGTase gene was tested for dextrinizing activity on an LB-starch agar plate. Cells with dextrinizing activity gave halo zone surrounding the colonies after exposure to a KI-I_2 indicator solution. Fig. 3.9 shows separately such activity from each mutant clone. Fig. 3.10 summarizes the halo zone assay of all the mutant transformants. All mutant CGTases are dextrinizing active whose activities are slightly higher than that of wild-type CGTase.

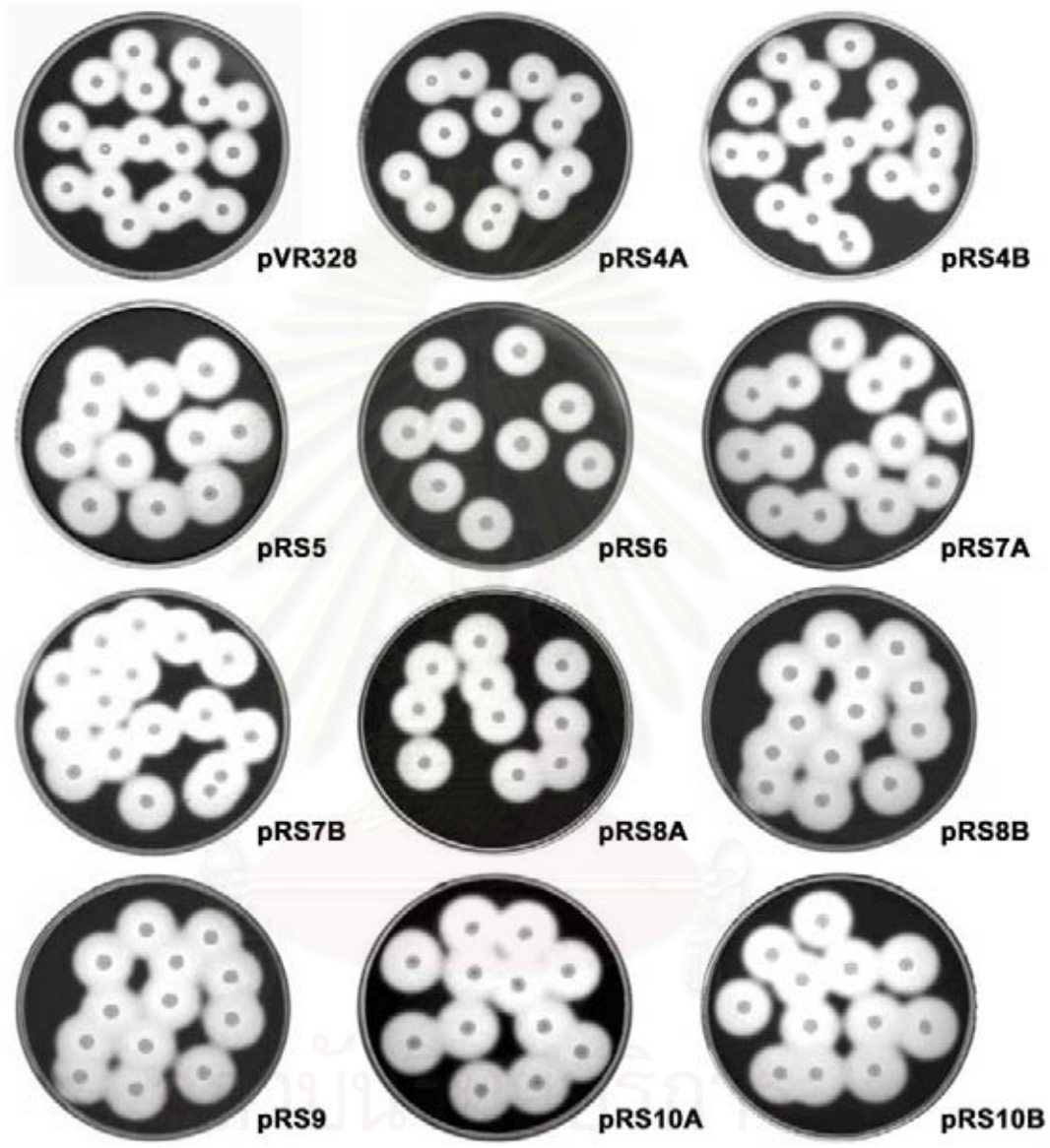

Fig. 3.9. Iodine test for dextrinizing activity of wild type and mutant CGTases. Clear zones surrounding the colonies indicate starch hydrolysis activity.

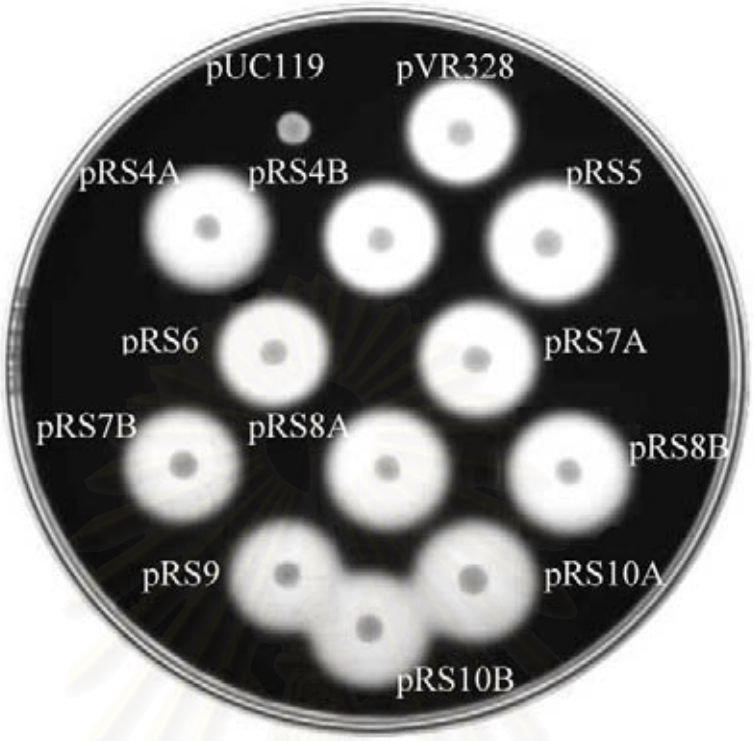

Fig. 3.10. Summary of the iodine test for dextrinizing activity of the wild type and the mutant CGTases. Clear zone surrounding the colonies indicates starch hydrolysis activity.

3.5.2 Dextrinizing activity assay at various temperatures

The crude enzymes in the culture supernatants of the transformants were also assayed for dextrinizing activity using the modified Fuwa method (Fuwa *et al*., 1954) (Table 3.1). The activities of the wild-type and mutant CGTases were measured at different temperatures. The profiles in Fig. 3.11 reveal 3 groups of mutant CGTases with different optimum temperatures. The mutant pRS6 (region III mutant) has more or less the same optimum temperature as the wild type at 65 ºC. The pRS4A (I_A), 4B (I_B), 5 (II), 8A (I_A+III), 8B (I_B+III) and 9 (II+III) have lower optimum temperature at about 60 ºC. The pRS7A (I_A+II), 7B (I_B+II), 10A (I_A+II+III) and 10B (I_B+II+III) seem to have lower optimum temperature than 60 ºC.

Table 3.1. Dextrinizing activity assay of wild-type and mutant CGTases at various temperatures.

Dextrinizing activity (unit/mg protein)						
Temperature (°C)	**40**	**50**	**60**	**65**	**70**	**80**
WT	1063.24	2714.54	6082.47	6759.62	6545.78	1437.46
pRS4A	2925.06	4128.89	5747.66	5665.69	3964.96	1275.55
pRS4B	1369.17	2484.70	2959.09	2855.76	2132.42	711.59
pRS5	3440.55	7146.41	9713.99	9405.88	5314.88	522.07
pRS6	1484.60	3015.15	5212.17	5736.14	5396.02	1259.38
pRS7A	1773.04	2741.47	3006.46	2204.25	884.11	19.27
pRS7B	1178.99	1653.32	1692.84	1327.56	760.55	128.12
pRS8A	1243.16	2568.37	4217.70	3778.70	2547.85	717.99
pRS8B	2616.62	4607.92	5840.84	5596.91	4204.34	975.69
pRS9	1120.54	2077.10	2916.89	2810.05	1383.91	360.26
pRS10A	1968.78	3427.56	3478.84	2592.75	1057.04	25.64
pRS10B	1719.08	3134.56	3692.54	2391.95	767.23	155.91

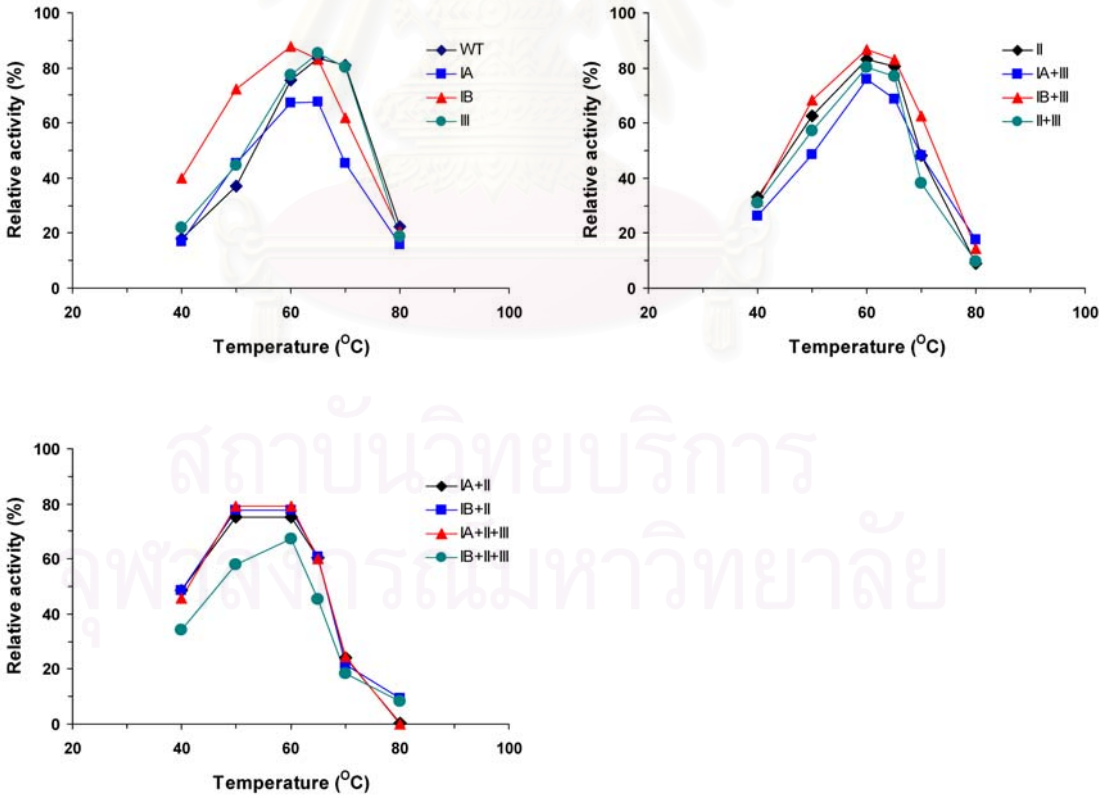

Fig. 3.11. Dextrinizing activity assay of the wild-type and mutant CGTases. The values are shown as relative activity at various temperatures. Each experiment was performed in duplicate.

3.5.3 Thermostability of the CGTases

The effect of temperature on the stability of CGTases was also investigated (Table 3.2). The activities of crude enzymes from the wild type and mutant CGTases were compared at various temperatures, and the percentages of relative activity are shown in Fig. 3.12. In general, the profiles indicate that all mutated CGTases exhibit lower stability than the wild-type CGTase except that of the pRS6 mutant, which has comparable stability to the wild-type CGTase.

Table 3.2. Specific activities of wild-type and mutant CGTases in the thermostability assay.

Thermostability activity (unit/mg protein)							
Temperature (°C)	**40**	**50**	**55**	**60**	**65**	**70**	**80**
WT	1416.13	1336.54	1183.92	1130.50	187.51	62.14	9.81
pRS4A	2997.89	2916.73	2619.15	1005.85	204.12	174.61	86.08
pRS4B	1475.68	1380.81	1313.37	602.39	171.46	129.17	50.29
pRS5	1965.04	1935.20	1793.83	219.91	190.06	164.93	47.12
pRS6	1348.97	1333.31	1266.20	1173.36	271.81	85.01	49.22
pRS7A	2790.61	2756.64	2465.44	317.89	116.48	75.23	2.43
pRS7B	1477.30	1396.29	1039.33	141.41	123.57	98.85	68.65
pRS8A	3580.52	3052.48	2953.65	1567.18	327.56	268.26	149.66
pRS8B	2841.23	2830.07	2693.81	1819.33	303.78	230.07	122.85
pRS9	1430.59	1385.85	1286.69	355.53	114.88	89.49	9.67
pRS10A	1677.51	1445.04	1179.56	305.65	167.89	74.62	31.57
pRS10B	2388.90	2100.87	1502.24	367.09	169.43	60.24	30.12

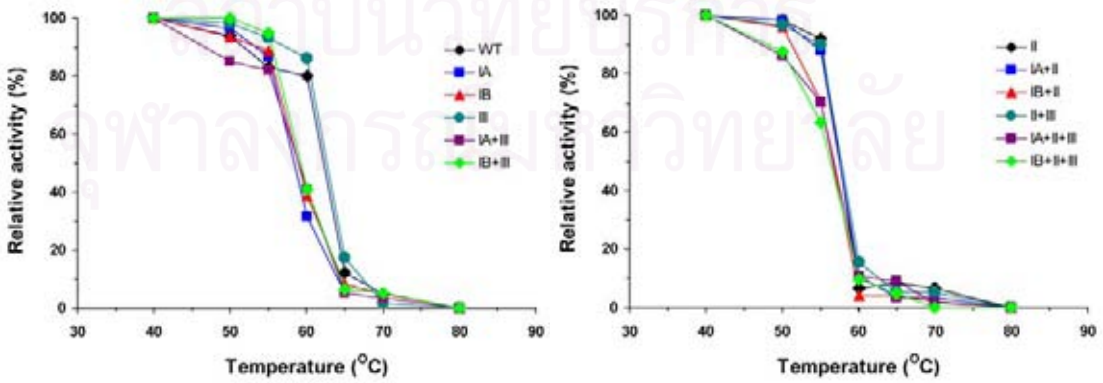

Fig. 3.12. Thermostability of the wild-type and mutant CGTases. The values are shown as relative activity at various temperatures. Each experiment was performed in duplicate.

3.5.4 Cyclodextrin forming activity

Cyclodextrin production by the mutant CGTases was determined by using HPLC. The crude enzyme from the culture of each mutant plasmid was incubated with soluble starch at 37 ºC for 12 hours. The reaction was terminated by boiling the mixture for 10 minutes. Then, 6U of glucoamylase were added, and the mixture was incubated for 4 hours to convert the linear oligosaccharides to glucose. All mutant enzymes exhibited the cyclodextrin forming activity.

The results were shown in Fig. 3.13. All the mutant enzymes produced β-CD as a major product and, hence, were β-CGTases. The pRS4A, 4B, 7A, 7B, 10A and 10B had increased proportion of α-CD production, while that of β-CD production was decreased significantly and the γ-CD production remained unchanged. The pRS5 had a proportion of α-, β-, γ-CD production similar to that of the wild type. The pRS6 had an increased proportion of α-CD, and a decreased proportion of γ-CD while the β-CD production remained more or less unchanged. The pRS8A and 8B had an increased proportion of α-CD and produced slightly lower both the proportions of β- and γ-CDs. The pRS9 had an increased proportion of β-CD production while the α- and γ-CD productions were decreased.

The ratio of cyclodextrins produced is an important characteristic of CGTases from various organisms. It was observed from the HPLC elution profiles that some of the mutant CGTases had altered product specificity. To measure the ratios, the peak area of each cyclodextrin in the HPLC profiles was determined. The cyclodextrin ratios were then calculated as percentage of the total peak areas of α-, β- and γ-CDs. Table 3.3 summarizes the two determinations of the cyclodextrin-forming activity.

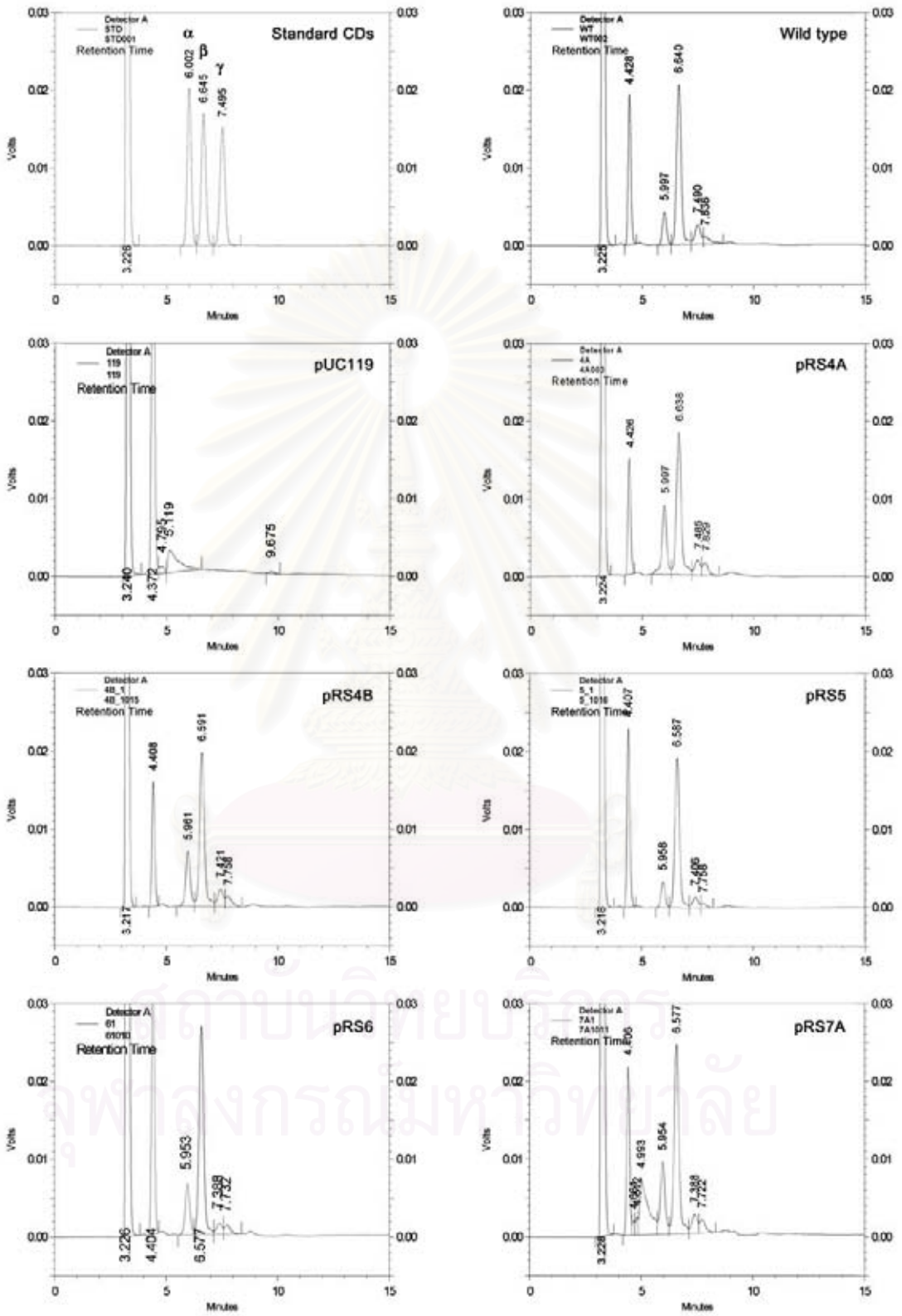

Fig. 3.13. HPLC profiles of cyclodextrins formed by the wild type and mutant CGTases.

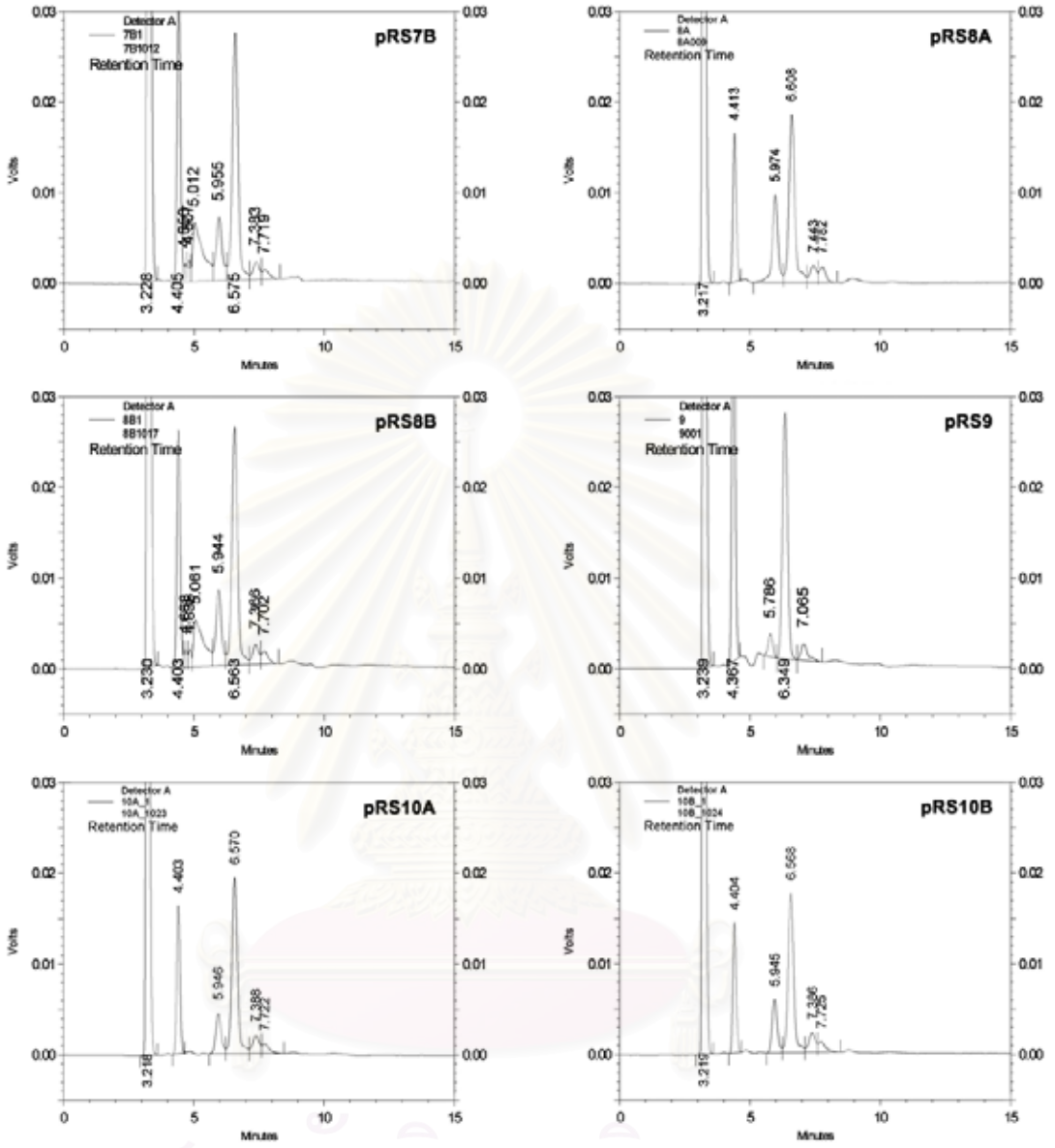

Fig. 3.13. (continued).

Table 3.3. Cyclodextrin-forming activity of the CGTases.

Plasmids	Cyclodextrin ratios, α:β:γ (%)	
	Experiment I	**Experiment II**
pVR328	12:79:9	13:75:12
pRS4A 	30:63:9	20:73:7
pRS4B 	23:68:9	28:64:8
pRS5 	12:81:7	17:77:6
pRS6 	18:77:5	18:76:6
pRS7A 	25:67:8	27:65:8
pRS7B 	20:74:6	24:66:10
pRS8A 	19:75:6	31:62:7
pRS8B 	23:71:6	20:71:9
pRS9 	7:85:8	9:84:7
pRS10A 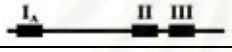	16:74:10	22:68:10
pRS10B 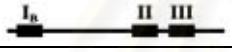	21:69:10	25:68:7

CHAPTER IV
DISCUSSION

A proper understanding of the molecular basis of thermal stability in protein could have important consequences for their application in a range of biotechnological processes. The availability of enzymes with the appropriate specificity and capable of surviving for long periods at elevated temperatures could lead to the creation of novel applications of enzyme-based technology in industries such as those involved in the processing of starch, paper, pulp or fibres (Flam, 1994; Adams and Kelly, 1995). The opportunities afforded by such applications have generated significant interest in the field and a large number of studies have been undertaken to unravel the molecular mechanisms involved in generating thermostable enzymes (Yip *et al*., 1998).

To improve thermostability of protein, a protein engineering approach is one of the many ways of studying. Engineering proteins for thermostability is a particular exciting and challenging field, as it is crucial for broadening the industrial use of recombinant proteins. Protein engineering is usually performed through site-directed mutagenesis, a favorite mode for genetic manipulation of the protein. Although the method is easy and highly useful, the rational mutagenesis requires detailed information on the tertiary structure and activities of the protein, the ability to predict the proper site of amino acid changes, and the intuition concerning the optimal amino acid to be changed (Kim *et al*., 2003).

One strategy for the identification of amino acid sequence portions that correlate with thermostability involves the comparison of both structures and amino acid sequences of the more stable proteins with the less stable ones. In this study, it is hypothesized that at a given position in an amino acid sequence alignment of homologous proteins, the respective consensus amino acid sequence of the thermostable enzymes contributes more than average to the stability of the protein than the nonconsensus amino acids. Consequently, substitution of the nonconsensus sequences in the less thermostable enzymes by those consensus amino acid sequences

of the thermostable enzymes may be a feasible approach for improving the thermostability (Lehmann and Wyss, 2001). Thus, the amino acid sequence alignments between CGTases from *Bacillus circulans* A11 and other thermophilic CGTases from *Thermoanaerobacterium thermosulfurigenes* EM1 and *B. stearothermophilus* NO2, *Thermoanaerobacter* sp. ATCC53627 and *B. stearothermophilus* ET1 were carried out. The amino acid sequences were downloaded from the GenBank. Fig. 3.1 shows the sequence comparison performed using ClustalX software. Besides the several homologous sequences scattered all over the protein sequences, there are four major regions, designated as regions I-IV, respectively at positions 89-94, 265-271, 333-339 and 538-540 (A11 CGTase numbering) (Fig. 3.1) that are different from those of the thermostable CGTases. The first region is located in domain B while the second and third regions are in domain A, the two domains of CGTases that constitute the active site. The forth region are in domain D. The differences in the first three regions may relate to the thermostability of CGTase. The forth region is most likely not relate to thermostability because it is not found in the thermostable CGTases as well as some ordinary CGTases. To study the involvement of the first three regions in the thermostability of protein, the A11 CGTase gene was mutated and genetically manipulated such that the three mutant genes as well as the genes containing the various combinations of the three mutated regions were obtained. Their activity, thermostability, and products were determined thereafter.

To create the three mutations in the A11 CGTase gene, four mutagenic primers were designed according to the amino acid regions in the CGTase that are different from those of thermostable CGTases. Two mutagenic primers were designed for region I because there were two amino acid sequence patterns in the thermostable CGTases. Primer A replaced the wild type sequence YSGVHN with DSTFGGS that also contained an insertion of one amino acid**,** and primer B replaced the YSGVHN with DASGS that delete the sequence by one amino acid. For the region II, primer C put the sequence VDPNNHY in place of ISPEYHQ. For the region III, the sequences among the thermostable CGTases were somewhat variable. Therefore, the primer D is designed as mixed oligonucleotides by which the wild type HTSNGDR is replaced by $Y^{I}/_{N}{}^{D}/_{G}EGD^{P}/_{T}$. The actual mutant region III read YIGEGDT. The mutagenesis

changed the three regions in A11 CGTase in favor of the amino acid sequences in thermostable CGTases (Fig. 3.5). The four mutated plasmids, pRS1A, 1B, 2 and 3, containing the mutant regions I_A, I_B, II and III, respectively, were obtained as shown in Fig. 3.4. The mutated sequences as well as the sequences nearby were confirmed by DNA sequencing. To avoid the possibility of mutation in other regions in the plasmids, the mutant regions were subcloned into the wild-type CGTase gene replacing the equivalent sequences. Various CGTase mutants were also constructed such that they contained all possible combinations of the mutated regions. These resulted in pRS4A, 4B, 5, 6, 7A, 7B, 8A, 8 B, 9, 10A and 10B which contained mutation regions I_A, I_B, II, III, I_A+II, I_B+II, I_A+III, I_B+III, II+III and I_A+II+III and I_B+II+III, respectively.

The three-dimensional structures of A11 β-CGTase (wild type CGTase) and the mutant CGTases were predicted by using homology modeling (www.cbs.dtu.dk/services/CPHmodels). Since the amino acid sequence of A11 CGTase is about 98% homologous to that of CGTase from *Bacillus* sp. 1011 (PDB 1I75), whose three-dimensional structure is already known, the predicted structure of the A11 CGTase was almost identical to that of CGTase from *Bacillus* sp. 1011. The predicted three-dimensional structures of pRS10A and 10B are also very similar to that of the wild type A11 CGTase (data not shown). Comparison of the conformation of the amino acids around the mutated residues showed clearly that no large structural rearrangements had taken place as a result of amino acid changes. The mutation regions were located on the surface of the enzyme (Fig. 4.1). Region I_A resided on the loop regions, which upon amino acid changes seemed to have no effect on the folding of the main chain α-helices and β-sheets. Likewise, the mutation region I_B, located at the same region as mutation region I_A, had no influences on the folding of the A11 CGTase. The mutation regions II and III also retained more or less the wild type conformation. These mutation regions resided outside the active site, and perhaps did not have any influence on the active site structure of the enzyme. This might be the reason why all the CGTase mutants retained their catalytic activity though some alterations in their activity did occur.

It was observed that all the mutants exhibited the dextrinizing activity. The *E. coli* JM109 transformants harboring each of the mutant CGTase gene were tested for

dextrinizing activity on the LB-starch agar plates (Figs. 3.9-3.10 and Table 3.1). The halos that appeared around the colonies after exposure to a KI-I_2 indicator solution showed that starch around the colonies had been degraded by the hydrolytic activity of the CGTases. At 40 ºC, CGTase mutants have slightly higher dextrinizing activity than the wild type (Fig. 3.10 and Table 3.1).

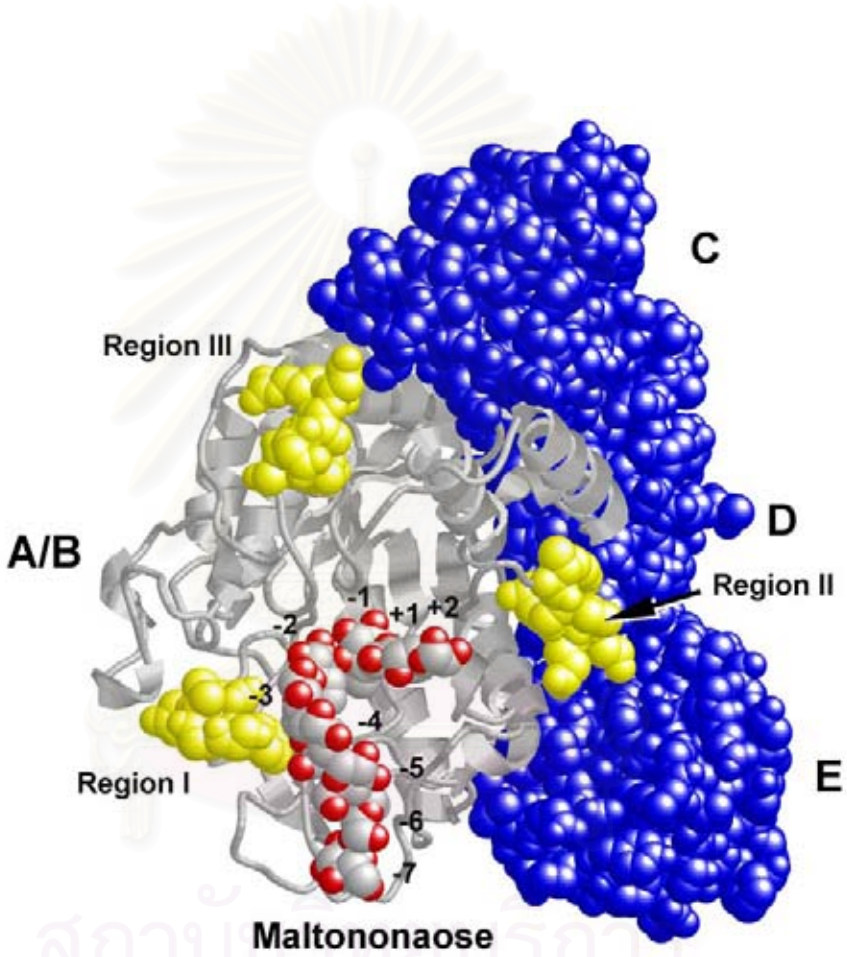

Fig. 4.1. Location of the three mutations regions relative to the binding subsites, presented by the maltononaose. The cocrystal structure of 251 CGTase (PDF 1CXK) is used as a model (Uitdehaag *et al.*, 1999).

By studying the crystal structure of CGTase from *Thermoanaerobacterium thermosulfurigenes* EM1, Knegtel et al. (1996) had observed 3 amino acid sequence regions that were different from those of *B. circulans* 251 CGTase (similar to A11 CGTase with ~86% homology). They hypothesized that the differences might

contribute to thermostability in EM1 CGTase. Two of the three regions were at the same positions as regions I and III in this study. The EM1 CGTase had a much higher hydrolytic activity than the 251 CGTase. Knegtel et al. (1996) speculated that the lack of Tyr89 in EM1 CGTase rendered it unable to sufficiently bind substrate strong enough for efficient cyclization. By changing the A11 CGTase region I amino acid sequence from YSGVHN to either DSTFGGS or DASGS, the Tyr89 (Y) were absent in the mutants. The results seemed to agree well with the speculation of Knegtel et al. (1996). However, other mutants with the Tyr89 also exhibited higher hydrolytic activity (see below). We argued here that the lacking of Tyr89 was not the major cause of higher hydrolytic activity in the A11 CGTase mutants in this study and perhaps not in EM1 CGTase either.

Mutations in regions II and III also resulted in higher dextrininzing activity in A11 CGTase. Region II was very close to the acceptor subsite +3 that was only found in *T. thermosulfurigenes* EM1 and other thermostable enzymes but not in other CGTases (Wind *et al.*, 1998; Leemhuis *et al.*, 2002), whereas region III was far away from the reactive cleft (Fig. 4.1). It had been proposed that the acceptor subsite +2 had the large effect on the hydrolytic activity of CGTase (Leemhuis *et al.*, 2003). One might think that mutation in region II (subsite +3), which was closed to subsite +2, could disturb the integrity of the subsite +2 and resulted in an increase in hydrolytic activity. However, the data presented here did not support the above notion since mutation in region III also resulted in comparable higher hydrolytic activity. The combination of mutant regions I+II, I+III, II+III and I+II+III also provided better dextrinizing activity than the wild type enzyme.

The crude mutant enzymes were prepared by culturing each clone in LB medium. The crude enzyme was obtained after the removal of cell pellet. The enzyme preparation was subjected to activity assay to determine the optimum temperature and thermostability. The optimum temperature was determined by measuring the dextrinizing activity at various temperatures from 40-80 ºC (Table 3.1 and Fig. 3.11). Mutation at regions I and II, but not III, slightly reduced the optimum temperatures. The combination of mutant regions, I+II and I+II+III, but not I+III or II+III, seemed to be the most deleterious. It was probably the combined effect of mutant regions I and II.

In literature, the stability of thermopilic proteins has been described in a number of ways, such as the temperature at which a protein is active (activity temperature), stable (stable temperature) or the half-life for certain duration of time. Much less frequently, the stability is described in terms of melting or mid-point transition temperature (*T*m) (Kumar *et al*., 2000). In this study, the thermostability of the mutant CGTases was described in terms of temperature as a function of the incubation time. It was determined by incubating the enzymes at various temperatures for 10 minutes, and then the residual starch-hydrolyzing activity of CGTase was assayed at certain optimum temperature, e.g. 40 ºC. The thermostability profiles in Fig. 3.12 reveal that mutations in regions I and II but not III reduce the thermostability of the enzyme. The combination of mutant regions does not seem to give more deleterious effect on the thermostability of the enzyme.

Leemhuis, *et al*. (2004) attempted to localize the amino acid regions involved in the thermostability of *B. circulans* 251 CGTase (251 CGTase) by comparing the three-dimensional structures of the five CGTases with known crystal structures and mutating the 251 CGTase in different regions to mimic the thermostable enzymes. The approach was very similar to this study. Five structural differences between the 251 CGTase and the EM1 CGTase were found in loop regions 88-94, 334-339, 494-498, 536-542, and 658-660 (A11 CGTase numbering). Two of them were identified in this study, namely regions I (89-94) and III (333-339). Almost identical change was made in region I_A (88-NYSGVNN to PDSTFGGS in 251 CGTase and 89-YSGVHN to DSTFGGS in A11 CGTase) but different change in region III (334-ASNANR to NGGST in 251 CGTase and 333-HTSNGDR to YIGEGDT in A11 CGTase). The changes in all three regions in A11 CGTase did not improve the thermostability of A11 CGTase. Similar to our finding, Leemhuis, *et al*. (2004) also found that all these changes towards thermostable CGTase had no effect on the thermostability of 251 CGTase.

Nevertheless, by providing a salt-bridge between positions 188 (N188D) and 192 (K192 or K192R), the half-life of the 251 CGTase at 60 ºC was moderately increased from 9.7 min to an average of 45 min whereas the EM1 CGTase retained full activity after 24 hours of incubation. Introduction of the other 3 salt-bridges found in the thermostable enzymes at positions R47-D89, D244-K510 and E275-K560 had

no or deleterious effect on the half-life of 251 CGTase. Likewise, the A11 CGTase also contained the N188 and K192, and would give similar result upon mutation to introduce the salt-bridge. Mutation in region I of A11 CGTase also resulted in Y89D that possibly formed salt-bridge with R47 and also did not improve the thermostability of the enzyme. Thus, it was reasonable to conclude that most of the structural and salt-bridge differences between the mesophilic CGTases and thermostable CGTases were not of primary importance for the thermostability.

To determine the CD forming activity by the mutant CGTases, the crude enzyme from each mutant plasmid was incubated with soluble starch at 37 ºC for 12 hours. The remaining oligosaccharides were digested with glucoamylase, and the reaction products were subjected to HPLC analysis. HPLC profiles of the CGTase reactions indicated that the mutant CGTases produced the cyclodextrins at various ratios, and some of them were different from that of the wild type (Fig. 3.13 and Table 3.3). For all the CGTase mutants, the proportion of γ–cyclodextrin produced was relatively unchanged or insignificantly decreased. The presence of region I mutants (pRS4A, 4B, 7A, 7B, 8A, 8B, 10A and 10B) resulted in an increase in α-cyclodextrin production with the expense of β-cyclodextrin production. Mutation in region II (pRS5) slightly decreased the proportion of γ-cyclodextrin and increased those of either β-cyclodextrin or α-cyclodextrin or both. Mutation in region III (pRS6) slightly decreased the proportion of γ-cyclodextrin and increased that of α-cyclodextrin. The mutants that had region I mutations in combination with the other two mutation regions (pRS7A, 7B, 8A, 8B, 10A and 10B) all had increased proportion of α-cyclodextrin. The influence of mutation in regions II and III was not obvious in these mutants; the proportion of γ-cyclodextrin was slightly decreased in pRS7A, 7B, 8A and 8B or unchanged in pRS10A and 10B. Interestingly, the combination of mutated regions II and III (pRS9) reduced the production of α-cyclodextrin, and increased that of β-cyclodextrin.

By using site-specific mutagenesis, van der Veen *et al*. (2000b) had reported that the mutations Y89D and S146P in 251 CGTase resulted in an increase in of α-cyclodextrin production. The Y89 was found to hydrophobically interact with the substrate in subsite –3, whereas the S146 was involved in hydrogen bonding in subsite -7. It was therefore concluded that changes in subsites –3 and –7 resulted in changes

in product specificity. In our study, mutation in region I, 89-YSGVHN to DSTFGGS in pRS4A and DASGS in pRS4B possibly created a salt-bridge with R47 like that found in thermostable enzymes but did not increase the thermostability of the enzyme. The mutation in turn resulted in a slight shift towards α-cyclodextrin production in agreement with the result of van der Veen *et al*. (2000b). Although the size of the loop region I in pRS4B was smaller, the observed cyclodextrin product ratio was relatively similar to that of pRS4A. On the other hand, Chotechuang (2003) had previously replaced the sequence around region I of the A11 CGTase from 87-INYSGVHN to HPGGF, which reduced the size of the loop region I by two amino acids more than the pRS4B CGTase. She found that the mutated enzyme produced mainly β-cyclodextrin and reduced the production of both the α- and γ-cyclodextrins. We argue here then that the subsite -3 was involved in the product specificity, not just for the α-cyclodextrin production but also β-cyclodextrin production. The size of the loop, as well as the hydrophobic interaction of Y89 with the substrate, might also play an important role in this respect.

For mutation in region II, it was interesting to find that the mutation in this region (pRS5) which resides very close to the supposedly subsite +3 had no influence on the product specificity. The acceptor binding subsite +3 was observed in *T. thermosulfurigenes* EM1 but not other mesophilic CGTases. Since the binding was very weak, it was believed to be less relevant to the enzyme activity (Wind *et al.*, 1998). Our result showed that the change in region III sequence of the A11 CGTase towards those of the thermostable enzymes provided very little effect, if any, on the enzyme activity. Contrarily, the mutation in region III (pRS6) which lay far away from the active site slightly increased the α-cyclodextrin production and slightly decreased the γ-cyclodextrin without affecting the β-cyclodextrin production. The influence of mutation in region III on the enzyme activity is not understood.

From our results, we had achieved our twofold goals. First, we were able to determine that the differences in the amino acid sequences, the structure as well, between the A11 CGTase and the thermostable CGTases were not the major determinants for thermostability of the enzyme. Second, we had tested the effect of mutation on the product specificity. We had found that mutations in region I and III but not II altered the enzyme product specificity. In other and our studies, we believed

that neither structural feature nor disulfide bridge alone was adequate for the thermostability of enzyme. Thermostability seemed rather to be caused by a complex and subtle interplay of many different factors, and it was often dependent on the function and environment of the protein (Fontana, 1991 and Jaenicke, 1991). The discrepancies in the relative importance of individual factors to stability arose from a combination of different molecular interactions that were differentially weighted on a case by case basis (Yip, 1998). Nevertheless, the key factor lies out there perhaps in the primary sequence and will soon be unveiled.

CHAPTER V
CONCLUSION

Amino acid sequence comparison between the *Bacillus circulans* A11 CGTase and the thermostable CGTases revealed four major different regions I, II, III and IV at position 89-94, 265-271, 333-339, and 538-540 (*B. circulans* A11 CGTase numbering), respectively. The amino acid sequences in the relevant regions I-III in catalytic domains A/B of β-CGTase from *B. circulans* A11 were mutated towards those of thermostable CGTases using the unique site elimination (USE) mutagenesis method. The CGTase mutants with various combinations of the three mutation regions were constructed and assayed for their activities and thermostability. It was found that mutations in the three mutation regions resulted in an increase in dextrinizing activity, a decrease in optimum temperature and no increase in thermostability. All CGTase mutants were active in CD-forming activity; all but one with altered product specificity.

REFERENCES

Adams, M.W.W., and Kelly, R.M. 1995. Enzymes from microorganisms in extreme environments. *Chem. Eng. News* 73:32-42.

Bar, R., and Ulitzur, S. 1994. Bacterial toxicity of cyclodextrins: Luminous *Escherichia coli* as model. *Appl. Microbiol. Biotechnol.* 41:574-577.

Bertoldo, C., and Antranikian, G. 2002. Starch-hydrolyzing enzymes from thermophilic archaea and bacteria. *Curr. Opin. Chem. Biol.* 6:151-160.

Biwer, A., Antranikian, G., and Heinzle, E. 2002. Enzymatic production of cyclodextrins. *Appl. Microbiol. Biotechnol.* 59:609-617.

Chakravarty, S., and Varadarajan, R. 2000. Elucidation of determinants of protein stability through genome sequence analysis. *FEBS Lett.* 470:65-69.

Chan, M.K., Mukund, S., Kletzin, A., Adams, M.W.W., and Rees, D.C. 1995. Structure of a hyperthermophilic tungstoperin enzyme, aldehyde ferredoxin oxidoreductase. *Science* 267:1463-1469.

Charoenlap, N., Dharmsthiti, S., Sirisansaneeyakul, S., and Lertsiri, S. 2004. Optimization of cyclodextrin production from sago starch. *Bioresour. Technol.* 92:49-54.

Chotechuang, N. 2003. *Mutagenesis of γ-cyclodextrin glucanotransferase gene from Bacillus circulans A11 that affects the γ-cyclodextrin production.* M.Sc. Thesis, Graduate School, Chulalongkorn University.

Chung, H.-J., Yoon, S.-H., Lee, M.-J., Kim, M.-J., Kweon, K.-S., Lee, I.-W., Kim, J.-W., Oh, B.-H., Lee, H.-S., Spiridonova, V.A., and Park, K.-H. 1998. Characterization of a thermostable cyclodextrin glucanotransferase isolated from *Bacillus stearothermophilus* ET1. *J. Agric. Food Chem.* 46:952-959.

Day, M.W., Hsu, B.T., Joshua-Tor, L., Park, J.B., Zhou, Z.H., Adams, M.W., and Rees, D.C. 1992. X-ray crystal structures of the oxidized and reduced forms of the rubredoxin from the marine hyperthermophilic archaebacterium *Pyrococcus furiosus*. *Protein Sci.* 1:1494-1507.

del Rio, G., Morett, E., and Soberon, X. 1997. Did cyclodextrin glycosyltransferases evolve from α-amylases?. *FEBS Lett.* 416:221-224.

Duchene, D. 1988. New trends in pharmaceutical applications of cyclodextrin inclusion compounds. In: Huber, O., and Szejtli J. (eds.), *Proceeding of the Forth International Symposium on Cyclodextrins*, pp. 265-275. Dordrecht, Kluwer Academic Publishers.

Flam, F. 1994. The chemistry of life at the margins. *Science* 265:471-472.

Fontanna, A. 1991. How nature engineers protein (thermo) stability. In: di Prisco, G. (ed.), *Life under extreme conditions*, pp. 89-113. Springer-Verlag Berlin-Heidelberg.

Fujimoto, Z., Takase, K., Doui, N., Momma, M., Matsumoto, T., and Mizuno, H. 1998. Crystal structure of a catalytic-site mutant alpha-amylase from *Bacillus subtilis* complexed with maltopentaose. *J. Mol. Biol.* 277:393-407.

Fujiwara, S., Kakihara, H., Sakaguchi, K., and Imanaka, T. 1992. Analysis of mutation in cyclodextrin glucanotransferase from *Bacillus stearothermophilus* which affect cyclization characteristics and thermostability. *J. Bacteriol.* 174:7478-7481.

Fuwa, H. 1954. A. new method for microdetermination of amylase activity by the use of amylases as the substrate. J. Biochem. 41:583-603.

Hobel, C.F.V. 2004. *Access to biodiversity and new genes from thermophiles by special enrichment methods.* Ph.D. Thesis. Department of Biology, Faculty of Sciences, University of Iceland.

Jaeniceke, R. 1991. Protein stability and molecular adaptation to extreme conditions. *Eur. J. Biochem.* 202:715-728.

Janecek, S. 1997. α-Amylase family: molecular biology and evolution. *Prog. Biophys. Mol. Biol.* 67:67-97.

Janecek, S. and Sevcik, J. 1999. The evolution of starch-binding domain. *FEBS Lett.* 456: 119-125.

Kaneko, T., Song, K.B., Hamamoto, T., Kudo, T., and Horikoshi, K. 1989. Construction of a chimeric series of *Bacillus* cyclomaltodextrin

glucanotransferases and analysis of the thermal stabilities and pH optima of the enzymes. *J. Gen. Microbiol.* 135:3447-3457.

Kim, Y.W., Choi, J.H., Kim, J.W., Park, C., Kim, J.W., Cha, H., Lee, S.B., Oh, B.H., Moon, T.W., and Park, K.H. 2003. Directed evolution of *Thermus* maltogenic amylase toward enhanced thermal resistance. Appl. Environ. Microbiol. 69:4866-4874.

Klein, C., and Schulz, G.E. 1991. Structure of cyclodextrin glycosyltransferase refined at 2.0 Å resolution. *J. Mol. Biol.* 217:737-750.

Knegtel, R.M.A., Strokopytov, B., Penninga, D., Faber, O.G., Rozeboom, H.J., Kalk, K.H., Dijkhuizen, L., and Dijkstra, B.W. 1995. Crystallographic studies of the interaction of cyclodextrin glycosyltransferase from *Bacillus circulans* strain 251 with natural substrates and products. *J. Biol. Chem.* 270:29256-29264.

Knegtel, R.M.A., Wind, R.D., Rozeboom, H.J., Kalk, K.H., Buitelaar, R.M., Dijkhuizen, L., and Dijkstra, B.W. 1996. Crystal structure at 2.3 Å resolution and revised nucleotide sequence of the thermostable cyclodextrin glycosyltransferase from *Thermoanaerobacterium thermosulfurigenes* EM1. *J. Mol. Biol.* 256:611-622.

Kubota, M., Matsuura, Y., Sakai, S., and Katsube, Y. 1991. Molecular structure of *B. stearothermophilus* cyclodextrin glucanotransferase and analysis of substrate binding site. Cited in Knegtel, R.M.A. *et al.* 1995. *J. Biol. Chem.* 270:29256-29264.

Kumar, S., Tsai, C.J., and Nussinov, R. 2000. Factors enhancing protein thermostability. *Protein Eng.* 13:179-191.

Lawson, C.L., van Montfort, R., Strokopytov, B., Rozeboom, H.J., Kalk, K.H., de Vries, G.E., Penninga, D., Dijkhuizen, L., and Dijkstra, B.W. 1994. Nucleotide sequence and X-ray structure of cyclodextrin glycosyltransferase from *Bacillus circulans* strain 251 in a maltose-dependent crystal form. *J. Mol. Biol.* 236:590-600.

Leemhuis, H., Kragh, K.M., Dijkstra B.W., and Dijkhuizen, L. 2003. Engineering cyclodextrin glycosyltransferase into a starch hydrolase with a high exo-specificity. *J. Biotechnol.* 103:203-212.

Leemhuis, H., Rozeboom, H.J., Dijkstra, B.W., and Dijkhuizen, L. 2004. Improved thermostability of *Bacillus circulans* cyclodextrin glycosyltransferase by the introduction of a salt-bridge. *Proteins* 54:128-134.

Lehmann, M., and Wyss, M. 2001. Engineering proteins for thermostability: the use of sequence alignments versus rational design and directed evolution. *Curr. Opin. Biotechnol.* 12:371-375.

McCoy, M. 1999. Cyclodextrins: great product seeks a market. *Chem. Eng. News* 77:25-27.

Mrabet, N.T., Van den Broeck, A., Van den brande, I., Stanssens, P., Laroche, Y., Lambeir, A.M., Matthijssens, G., Jenkins, J., Chiadmi, M., van Tilbeurgh, H., *et al.* 1992. Arginine residues as stabilizing elements in proteins. *Biochemistry* 31:2239-2253.

Niehaus, F., Bertoldo, C., Kahler, M., and Antranikian, G. 1999. Extremophiles as a source of novel enzymes for industrial application. *Appl. Microbiol. Biotechnol.* 51:711-729.

Penninga, D. 1996. *Protein engineering of cyclodextrin glycosyltransferase from Bacillus circulans strain 251.* Ph.D. Thesis, University of Groningen.

Penninga, D., van der Veen, B.A., Knegtel, R.M.A., van Hijum, S.A.F.T., Rozeboom, H.J., Kalk, K.H., Dijkstra, B.W. and Dijkhuizen, L. 1996. The raw starch binding domain of cyclodextrin glucanotransferase from *Bacillus circulans* strain 251. *J. Biol. Chem.* 271:32777-32784.

Pongsawasdi, P., and Yagisawa, M. 1987. Screening and identification of a cyclomaltodextrin glycanotransferase producing bacteria. *J. Ferment. Technol.* 65:463-467.

Rashid, N., Cornista, J., Ezaki, S., Fukui, T., Atomi, H., and Imanaka, T. 2002. Characterization of an archaeal cyclodextrin glucanotransferase with a novel C-terminal domain. *J. Bacteriol.* 184:777-784.

Riisgaard, S. 1990. The enzyme industry and modern biotechnology. In: Christiansen, C., Munck, L., and Villadsen, J. (eds.), *Proceedings of the fifth European congress on biotechnology*, pp. 31-40. Copenhagen, Denmark: Munksgaard International Publishers.

Rimphanitchayakit, V., Tonozuka, T., and Sakano, Y. 2005. Construction of chimeric cyclodextrin glucanotransferases from *Bacillus circulans* A11 and *Paenibacillus macerans* IAM1243 and analysis of their product specificity. Carbohydr Res. 340:2279-2289.

Strokopytov, B., Knegtel, R.M., Penninga, D., Rozeboom, H.J., Kalk, K.H., Dijkhuizen, L., and Dijkstra, B.W. 1996. Structure of cyclodextrin glycosyltransferase complexed with a maltononaose inhibitor at 2.6 Å resolution. Implications for product specificity. *Biochemistry.* 35:4241-4249.

Strop, P., and Mayo, S.L. 2000. Contribution of surface salt bridges to protein stability. *Biochemistry* 39:1251-1255.

Svensson, B., Jespersen, H., Sierks, M.R., and Macgregor, E.A. 1989. Sequence homology between putative raw-starch binding domains from different starch-degrading enzymes. *Biochem. J.* 264:309-311.

Szejtli, J. 1998. Introduction and general overview of cyclodextrin chemistry. *Chem. Rev.* 98:1743-1754.

Thompson, J.D., Plewniak, F., and Poch, O. 1999. A comprehensive comparison of multiple sequence alignment programs. *Nucleic Acids Res.* 27:2682-2690.

Tonkova, A. 1998. Bacterial cyclodextrin glucanotransferase. *Enzyme Microb. Technol.* 22:678-686.

Uitdehaag J.C.M. and Dijkstra B.W. 1998. A strategy for engineering thermostability: the case of cyclodextrin glycosyltransferase. In: Ballesteros, A., Plou, F.J., Iborra, J.L., and Halling, P.J. (eds.), *Stability and stabilization of biocatalysts*, pp. 317-323. Elsevier Amsterdam.

Uitdehaag, J.C., Mosi, R., Kalk, K.H., van der Veen, B.A., Dijkhuizen, L., Withers, S.G., and Dijkstra, B.W. 1999. X-ray structures along the reaction pathway of cyclodextrin glycosyltransferase elucidate catalysis in the alpha-amylase family. *Nat. Struct. Biol.* 6:432-436.

Uitdehaag, J.C.M., van der Veen, B.A., Dijkhuizen, L., and Dijkstra, B.W. 2002. Catalytic mechanism and product specificity of cyclodextrin glycosyltransferase, a propotypical transglycosylase from the α-amylase family. *Enzyme Microb. Technol.* 30:295-304.

van der Veen, B.A., Uitdehaag, J.C.M., Dijkstra, B.W., and Dijkhuizen, L. 2000a. Engineering of cyclodextrin glycosyltransferase reaction and product specificity. *Biochim. Biophys. Acta.* 1543:336-360.

van der Veen, B.A., Uitdehaag, J.C.M., Penninga, D., van Alebeek, G.J., Smith, L.M., Dijkstra, B.W., and Dijkhuizen, L. 2000b. Rational design of cyclodextrin glycosyltransferase from *Bacillus circulans* strain 251 to increase alpha-cyclodextrin production. *J. Mol. Biol.* 296:1027-1038.

Wind, R.D., Liebl, W., Buitelaar, R.M., Penninga, D., Spreinat, A., Dijkhuizen, L., and Bahl, H. 1995. Cyclodextrin formation by the thermostable alpha-amylase of *Thermoanaerobacterium thermosulfurigenes* EM1 and reclassification of the enzyme as a cyclodextrin glycosyltransferase. *Appl. Environ. Microbiol.* 61:1257-1265.

Wind, R.D., Uitdehaag, J.C., Buitelaar, R.M., Dijkstra, B.W., and Dijkhuizen, L. 1998. Engineering of cyclodextrin product specificity and pH optima of the thermostable cyclodextrin glycosyltransferase from *Thermoanaerobacterium thermosulfurigenes* EM1. *J. Biol. Chem.* 273:5771-5779.

Yamamoto, T., Shiraki, K., Fujiwara, S., Takagi, M., Fukui, K., and Imanaka, T. 1999. In vitro heat effect on functional and conformational changes of cyclodextrin glucanotransferase from hyperthermophilic archaea. *Biochem. Biophys. Res. Commun.* 265:57-61.

Yip, K.S., Britton, K.L., Stillman, T.J., Lebbink, J., de Vos, W.M., Robb, F.T., Vetriani, C., Maeder, D., and Rice, D.W. 1998. Insights into the molecular basis of thermal stability from the analysis of ion-pair networks in the glutamate dehydrogenase family. *Eur. J. Biochem.* 255:336-346.

APPENDICES

APPENDIX A

1. Reagents for plasmid preparation

1.1. Lysis solution: 10 mL

50% Glucose	2	mL
0.5 M EDTA	0.2	mL
1 M Tris-HCl (pH 8.0)	0.25	mL
ddH_2O	7.55	mL

1.2. Alkaline SDS solution: 10 mL

5% SDS	2	mL
5 N NaOH	0.4	mL
ddH_2O	7.6	mL

1.3. Hight salt solution: 3 M Sodium acetate (pH 5.2)

$NaOAc.3H_2O$	408.1	g
ddH_2O	700	mL

Adjust pH to 5.2 with glacial acetic and adjust the volume to 1 litre with water.

2. Other reagents for preparation

2.1. RNase A solution

Dissolve RNase A (pancreatic) at a concentration of 10 mg/mL in 10 mM Tris-HCl (pH 7.5), 15 mM NaCl, then heat at 100 ºC, 15 min, cool slowly at room temperature, aliquot, and store at -20 ºC.

2.2. 10% Glycerol

Glycerol	10	mL
Water	90	mL

2.3. 5× TBE buffer (for agarose gel electrophoresis)

Tris-base	54	g
Boric acid	27.5	g
0.5 M EDTA (pH 8)	20	mL

2.4. 0.5 M EDTA

EDTA	186.1	g
Water	1000	mL

Dissolve EDTA in 800 mL water and adjust pH to 8.0 with NaOH before adjusting volume to 1 litre, and then autoclave.

2.5. 1M Tris-HCl

Tris-base	121.1	g
Water	1000	ml

Adjust pH to 7-8 before adjusting volume to 1 litre, and then autoclave.

2.6. 5% SDS (store at room temperature)

SDS	5	g
Water	100	mL

2.7. 5N NaOH

NaOH	20	g
Water	100	mL

Dissolve NaOH in 70 ml water before adjusting volume to 100 mL

2.8. Loading buffer (for agarose gel electrophoresis)

Glycerol	20	mL
Bromophenol blue	4	mg
Water	80	mL

2.9. Coomassie blue reagent

Coomassie blue G 250	50	mg
95% Ethanol	25	mL
85% H_3PO_4	50	mL

Adjust volume to 500 mL with water.

APPENDIX B

Standard curve for protein determination by Coomassie blue method.

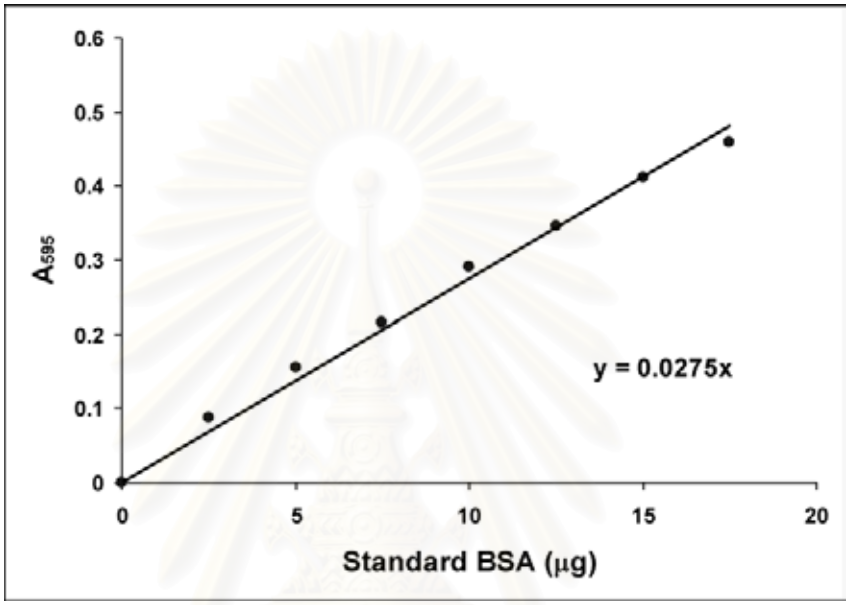

APPENDIX C

The restriction map of pVR328, showing the restriction sites used in this project.